

Longitudinal Modeling of Age-Dependent Latent Traits with Generalized Additive Latent and Mixed Models

Øystein Sørensen¹, Anders M. Fjell^{1,2}, and Kristine B. Walhovd^{1,2}

¹*Center for Lifespan Changes in Brain and Cognition, Department of Psychology, University of Oslo, Norway*

²*Department of Radiology and Nuclear Medicine, Oslo University Hospital, Norway*

Abstract

We present generalized additive latent and mixed models (GALAMMs) for analysis of clustered data with responses and latent variables depending smoothly on explanatory variables. An iterative profile likelihood algorithm is proposed, which combines existing efficient software for generalized additive mixed models with a quasi-Newton step. We derive asymptotic standard errors of both smooth and parametric terms. The models developed were motivated by applications in cognitive neuroscience, and three case studies are presented. First, we show how GALAMMs can successfully model the complex lifespan trajectory of latent episodic memory, using longitudinal data with five test scores at each timepoint. Next, we extend the model to study the joint trajectories of episodic and working memory across life. Finally, we study the effect of socioeconomic status on brain structure, using data on education and income together with hippocampal volumes estimated by magnetic resonance imaging. By combining semiparametric estimation with latent variable modeling, GALAMMs allow a more realistic representation of how brain and cognition vary across the lifespan, while simultaneously estimating latent traits from measured items. Simulation experiments suggest that model estimates are accurate even with moderate sample sizes.

Keywords: generalized additive mixed models, item response theory, latent variable modeling, cognitive neuroscience, structural equation modeling.

1 Introduction

Generalized linear mixed models (GLMMs) and nonlinear mixed models are widely used whenever observations can be divided into meaningful clusters. However, they require the parametric form of the effects to be exactly specified, and in many applications this may be impractical or not possible. For example,

when studying how the human brain changes over the lifespan, volumes of different brain regions exhibit distinctive trajectories, differing with respect to rate of increase during childhood, age at which maximum is attained, and rate of decline in old age (Sørensen et al., 2021). Similarly, domain-specific cognitive abilities follow unique lifespan trajectories, with traits like episodic memory and processing speed reaching a peak in the early adulthood, while acquired knowledge like vocabulary peaks in late adulthood (McArdle et al., 2002). Generalized additive (mixed) models (GAMs/GAMMs) (Hastie and Tibshirani, 1986; Wood, 2017) flexibly estimate nonlinear relationships by a linear combination of known basis functions subject to smoothing penalty, and are ideally suited to these applications.

Both GLMMs and GAMMs can be used for analyzing multivariate response data (Fieuws and Verbeke, 2006; Wood et al., 2016), allowing estimation of correlated change across multiple processes. However, when multivariate responses are considered noisy realizations of lower-dimensional latent variables, GLMMs and GAMMs essentially assume a parallel measurement model (Novick, 1966), in which the coefficients relating latent to observed variables are known at fixed values. Originating from confirmatory factor analysis, structural equation models (SEMs) offer more flexible latent variable modeling. The measurement part of a SEM regresses multivariate responses on a lower number of latent variables, while the structural part models how the latent variables are correlated and how they depend on explanatory variables. Extensions of the SEM framework include nonlinear models (Arminger and Muthén, 1998; Busemeyer and Jones, 1983; Kenny and Judd, 1984; Lee and Zhu, 2000), semiparametric latent basis models (Meredith and Tisak, 1990), and models for categorical and ordinal response data (Muthén, 1984). Despite these advances, SEMs have limitations in terms of incorporating explanatory variables and analyzing unbalanced or multilevel data. Several proposed models bring SEMs closer to the flexibility of GLMMs, while retaining their ability to model latent variables (Mehta and Neale, 2005; Muthén, 2002; Oud and Jansen, 2000; Proust-Lima et al., 2013; Rabe-Hesketh et al., 2004a). In particular, generalized linear latent and mixed models (GLLAMMs) (Rabe-Hesketh et al., 2004a) exploit the equivalence between random effects and latent variables to model latent and explanatory variables varying at any level. GLLAMMs are nonlinear hierarchical models whose likelihood function can be estimated with numerical integration (Rabe-Hesketh et al., 2005), and many special cases of GLLAMMs can be computed with a profile likelihood approach combining existing GLMM software with a general purpose optimization routine (Jeon and Rabe-Hesketh, 2012; Rockwood and Jeon, 2019). As GLLAMMs model the observed responses with an exponential family distribution, they are not limited to factor analytic measurement models, and contain important psychometric methods like item response models and latent class models as special cases.

While nonlinear modeling is straightforward with GLLAMMs, as with GLMMs the functional parametric forms are assumed known. In this paper, we introduce generalized additive latent and mixed models

(GALAMMs), a semiparametric extension of GLLAMMs in which both the linear predictor and latent variables may depend smoothly on observed variables. Utilizing the mixed model view of smoothing (Ruppert et al., 2003; Wood, 2017), we show that any GALAMM can be represented as a GLLAMM, with smoothing parameters estimated by maximum likelihood. This allows profile likelihood estimation of GALAMMs, combining existing GAMM software with a general purpose optimization routine. Asymptotic standard errors and confidence bands of estimated smooth functions can be computed by extending existing methods for GAMMs (Marra and Wood, 2012; Ruppert et al., 2003). The proposed methods are similar to fully Bayesian approaches to semiparametric latent variable modeling (Fahrmeir and Raach, 2007; Song and Lu, 2010; Song et al., 2013, 2014), all of which have been limited to latent variables varying at a single level. In contrast, GALAMMs allow multilevel modeling with any number of levels, and both nested and crossed random effects.

The paper proceeds as follows. In Section 2 we start by presenting the general framework, then show how GALAMMs can be represented as GLLAMMs, and derive the reduced form of the resulting models. We then present a profile likelihood algorithm for maximum likelihood estimation and derive asymptotic standard errors for the estimated parameters and smooth functions. In Section 3 we present three example applications from cognitive neuroscience. We first illustrate how the lifespan trajectory of episodic memory can be estimated from longitudinal data, combining the results of multiple cognitive tests taken at each timepoint. Next, the model is extended to jointly study lifespan trajectories of episodic and working memory, and finally we study how socioeconomic status is associated with hippocampal volume across the lifespan. Each application in Section 3 is followed by simulation experiments closely following the data structure and parameters of the real analysis. We discuss the results in Section 4.

2 Generalized Additive Latent and Mixed Models

We consider multilevel models with components varying at L levels, and use generalized random coefficient notation (Skrondal and Rabe-Hesketh, 2004, Ch. 4), which is here briefly reviewed. The multivariate responses for all units are stacked in a vector \mathbf{y} of length n , whose elements y_i are the elementary units of observation, varying at level 1. Latent variables vary at level 2 or higher, and $\boldsymbol{\eta}^{(l)}$ denotes a vector of M_l latent variables varying at level l , with m th element $\eta_m^{(l)}$. The vector of all latent variables belonging to the j th level-2 unit is

$$\boldsymbol{\eta}_j = \left[\boldsymbol{\eta}_{jk\dots z}^{(2)'} , \boldsymbol{\eta}_{k\dots z}^{(3)'} , \dots , \boldsymbol{\eta}_z^{(L)'} \right]', \quad (1)$$

and $\boldsymbol{\eta}_j^{(l+)} = (\boldsymbol{\eta}_{j\dots z}^{(l)'} , \dots, \boldsymbol{\eta}_z^{(L)'})'$ denotes elements of $\boldsymbol{\eta}_j$ varying at level l or higher. Similarly, \mathbf{w}_j denotes explanatory variables on which the latent variables depend, and we assume these variables are permuted in such a way that we can write

$$\mathbf{w}_j = \left[\mathbf{w}_{jk\dots z}^{(2)'} , \mathbf{w}_{k\dots z}^{(3)'} , \dots, \mathbf{w}_z^{(L)'} \right]', \quad (2)$$

where $\mathbf{w}_{jk\dots z}^{(2)}$ are variables varying at level 2, $\mathbf{w}_{k\dots z}^{(3)}$ are variables varying at level 3, and so on. Whereas latent variables are required at all levels, any element in (2) may be empty.

2.1 Model Framework

We assume a response distribution given by an exponential family with density

$$f(y_i|\theta_i, \phi) = \exp \left\{ \frac{y_i\theta_i - b(\theta_i)}{\phi} + c(y_i, \phi) \right\}, \quad (3)$$

where θ_i is a function of the mean $\mu_i = g^{-1}(\nu_i)$, $g^{-1}(\cdot)$ being the inverse of link function $g(\cdot)$, and ν_i a linear predictor. The linear predictor for level-1 unit i is related to explanatory variables \mathbf{x}_i and latent variables through the measurement model

$$\nu_i = \sum_{s=1}^S f_s(\mathbf{x}_i) + \sum_{l=2}^L \sum_{m=1}^{M_l} \eta_m^{(l)} \mathbf{z}_{mi}^{(l)'} \boldsymbol{\lambda}_m^{(l)}, \quad (4)$$

where $\{f_s(\mathbf{x}_i)\}_{s=1}^S$ are functions of one or more elements of explanatory variables \mathbf{x}_i . We omit higher-level subscripts, but note that $\eta_m^{(l)}$ is an element of $\boldsymbol{\eta}_j$ in (1) varying at level l , with j denoting the level-2 unit to which the i th level-1 unit belongs. The term $\mathbf{z}_{mi}^{(l)'} \boldsymbol{\lambda}_m^{(l)}$ relates the m th latent variable at level l to the i th measurement, where $\boldsymbol{\lambda}_m^{(l)}$ contains parameters to be estimated and $\mathbf{z}_{mi}^{(l)}$ are explanatory variables varying at level l or higher. Each function $f_s(\cdot)$ in (4) is a linear combination of B_s basis functions

$$f_s(\mathbf{x}_i) = \sum_{k=1}^{B_s} \omega_{ks} b_{ks}(\mathbf{x}_i), \quad s = 1, \dots, S, \quad (5)$$

with weights ω_{ks} . The basis functions are assumed to be cubic regression splines or thin-plate regression splines (Wood, 2003), and we assume multivariate smooth functions are constructed according to Wood et al. (2013).

The structural part of the model is

$$\boldsymbol{\eta}_j = \mathbf{B}\boldsymbol{\eta}_j + \mathbf{h}(\mathbf{w}_j) + \boldsymbol{\zeta}_j, \quad (6)$$

where \mathbf{B} is an $M \times M$ matrix of coefficients for regressions between the latent variables, with $M = \sum_{l=2}^L M_l$. Following Rabe-Hesketh et al. (2004a) we assume non-recursive relations between latent variables, and require that a latent variable varying at level l can only depend on latent variables varying at level l or higher. By a permutation of the latent variables varying at each level, it follows that \mathbf{B} is strictly upper diagonal (Skrondal and Rabe-Hesketh, 2004, p. 109). We have also defined the vector valued function $\mathbf{h}(\mathbf{w}_j)$, itself composed of $L - 1$ vector-valued functions $\mathbf{h}_l\{\mathbf{w}_j^{(l+)}\}$ with M_l elements, one for each latent variable varying at level l :

$$\mathbf{h}(\mathbf{w}_j) = \begin{bmatrix} \mathbf{h}_2\{\mathbf{w}_j^{(2+)}\} \\ \mathbf{h}_3\{\mathbf{w}_j^{(3+)}\} \\ \vdots \\ \mathbf{h}_L\{\mathbf{w}_j^{(L)}\} \end{bmatrix}, \text{ with } \mathbf{h}_l\{\mathbf{w}_j^{(l+)}\} = \begin{bmatrix} h_{l1}\{\mathbf{w}_j^{(l+)}\} \\ h_{l2}\{\mathbf{w}_j^{(l+)}\} \\ \vdots \\ h_{l,M_l}\{\mathbf{w}_j^{(l+)}\} \end{bmatrix}, \quad l = 2, \dots, L,$$

where $h_{lm}\{\mathbf{w}_j^{(l+)}\}$ is a smooth function of a subset of $\mathbf{w}_j^{(l+)}$ predicting the value of $\eta_m^{(l)}$. By this definition, latent variables varying at level l may only depend on explanatory variables varying at level l or higher. Each $h_{lm}(\cdot)$ is a linear combination of D_{lm} basis functions $d_{klm}(\cdot)$,

$$h_{lm}\{\mathbf{w}_j^{(l+)}\} = \sum_{k=1}^{D_{lm}} \kappa_{klm} d_{klm}\{\mathbf{w}_j^{(l+)}\}, \quad (7)$$

with weights κ_{klm} . If $\eta_m^{(l)}$ does not depend on explanatory variables, we set $D_{lm} = 0$, and if $\eta_m^{(l)}$ depends on $S_{lm} > 1$ smooth functions it can be extended to $\sum_{s=1}^{S_{lm}} h_{slm}(\cdot)$, but we omit this for ease of exposition. To complete the specification of the structural model (6), ζ_j is a vector of normally distributed disturbances, $\zeta_j \sim N(\mathbf{0}, \Psi)$, with block-diagonal covariance matrix $\Psi = \text{diag}(\Psi^{(2)}, \dots, \Psi^{(L)})$, $\Psi^{(l)}$ being the covariance of disturbances at level l .

2.2 Mixed Model Representation

We assume that each smooth function has an associated smoothing penalty. For example, with squared second derivative penalization, terms of the form $\gamma_s^f \int f_s''(\mathbf{u})^2 d\mathbf{u}$ and $\gamma_{lm}^h \int h_{lm}''(\mathbf{u})^2 d\mathbf{u}$ are added to the log-likelihood. Here \mathbf{u} denotes the vector of variables on which the respective function depends, and the limits of integration are the upper and lower limits of the sample values of these variables. The smoothing parameters γ_s^f and γ_{lm}^h can be viewed as inverse variance components and estimated with maximum likelihood by GLMM software (see Ruppert et al. (2003), Wood (2017) and the references therein). This mixed model view of smoothing turns out to be useful also for GALAMMs, as it lets the model be represented by a GLLAMM with smoothing parameters defining an additional top level $L + 1$ of latent variables with diagonal covariance

matrix $\Psi^{(L+1)}$. When a smooth term depends on multiple variables with different scales (e.g., position in kilometers and time in seconds), scale invariant tensor product smooths are useful (Wood et al., 2013). For example, if the argument \mathbf{x} to $f_s(\mathbf{x})$ can be naturally divided into components \mathbf{x}_1 and \mathbf{x}_2 , whose elements are measured on the same scale, we define $f_s(\mathbf{x})$ as a tensor product of marginal smooths $f_{s1}(\mathbf{x}_1)$ and $f_{s2}(\mathbf{x}_2)$, following Wood et al. (2013).

2.2.1 Measurement Model

Consider a smooth term $f_s(\cdot)$ in the measurement model (4), and let $\tilde{\mathbf{X}}_s$ be a matrix whose columns equal this term's basis functions evaluated over the whole sample, i.e.,

$$\tilde{\mathbf{X}}_s = \begin{bmatrix} b_{1s}(\mathbf{x}_1) & \dots & b_{B_s,s}(\mathbf{x}_1) \\ \vdots & & \vdots \\ b_{1s}(\mathbf{x}_n) & \dots & b_{B_s,s}(\mathbf{x}_n) \end{bmatrix}. \quad (8)$$

Defining $\boldsymbol{\omega}_s = (\omega_{1s}, \dots, \omega_{B_s,s})'$, the sample values of the smooth term are given by $\mathbf{f}_s = \tilde{\mathbf{X}}_s \boldsymbol{\omega}_s$. We express the smoothing penalty in terms of a penalty matrix \mathbf{P}_s , e.g., $\gamma_s^f \int f_s''(\mathbf{u})^2 d\mathbf{u} = \gamma_s^f \boldsymbol{\omega}_s' \mathbf{P}_s \boldsymbol{\omega}_s$. Considering the penalty as expressing an assumption of smoothness of $f_s(\cdot)$, we may view it as resulting from a Bayesian prior distribution $\boldsymbol{\omega}_s \sim N(\mathbf{0}, \mathbf{P}_s^- / \gamma_s^f)$, where \mathbf{P}_s^- is the pseudoinverse of \mathbf{P}_s . Through an eigendecomposition, we can express \mathbf{f}_s as

$$\mathbf{f}_s = \mathbf{X}_s \boldsymbol{\beta}_s + \mathbf{Z}_s \boldsymbol{\eta}_s^f, \quad (9)$$

where \mathbf{X}_s spans the nullspace of \mathbf{P}_s and \mathbf{Z}_s spans the column space of \mathbf{P}_s , $\boldsymbol{\beta}_s$ are fixed effects and $\boldsymbol{\eta}_s^f \sim N(\mathbf{0}, \mathbf{I} / \gamma_s^f)$ are random effects. For tensor products of v marginal smooths constructed following Wood et al. (2013), \mathbf{Z}_s and $\boldsymbol{\eta}_s^f$ in (9) are replaced by $2^v - 1$ random effect matrices and coefficient vectors, each with its own variance component γ_{sj}^f , $j = 1, \dots, 2^v - 1$, and diagonal covariance matrix $\mathbf{I} / \gamma_{sj}^f$. Repeating this eigendecomposition for all S smooth functions in the measurement model (4) we can define the matrix $\mathbf{X} = [\mathbf{X}_1, \dots, \mathbf{X}_S]$ associated with fixed effects $\boldsymbol{\beta} = (\boldsymbol{\beta}'_1, \dots, \boldsymbol{\beta}'_S)'$ and the matrix

$$\mathbf{Z}^f = [\mathbf{Z}_1, \dots, \mathbf{Z}_S] \quad (10)$$

associated with random effects

$$\boldsymbol{\eta}^f = \left(\boldsymbol{\eta}_1^{f'}, \dots, \boldsymbol{\eta}_S^{f'} \right)'. \quad (11)$$

Let M_{L+1}^f denote the number of elements in $\boldsymbol{\eta}^f$, and \mathbf{x}_i the i th row of \mathbf{X} .

Some special cases captured by this formulation are worth pointing out. When $f_s(\cdot)$ is an intercept or a linear regression term and second derivative penalization is used, the whole function lies in the penalty nullspace, and we obtain $\mathbf{f}_s = \mathbf{X}_s \boldsymbol{\beta}_s$. For a fully penalized term, on the other hand, e.g. with a ridge-type penalty, the whole function lies in the penalty range space and we obtain $\mathbf{f}_s = \mathbf{Z}_s \boldsymbol{\eta}_s^f$.

2.2.2 Structural Model

A similar transformation applies to the smooth terms in the structural model (6). From (7) define the vector of spline coefficients $\boldsymbol{\kappa}_{lm} = (\kappa_{1lm}, \dots, \kappa_{D_{lm},l,m})'$ of the l th smooth function predicting the m th latent variable, and let n_2 denote the total number of level-2 units. We define

$$\tilde{\mathbf{W}}_{lm} = \begin{bmatrix} d_{1lm}(\mathbf{w}_1) & \dots & d_{D_{lm},l,m}(\mathbf{w}_1) \\ \vdots & & \vdots \\ d_{1lm}(\mathbf{w}_{n_2}) & \dots & d_{D_{lm},l,m}(\mathbf{w}_{n_2}) \end{bmatrix},$$

such that the sample values of $h_{lm}(\cdot)$ are $\mathbf{h}_{lm} = \tilde{\mathbf{W}}_{lm} \boldsymbol{\kappa}_{lm}$. Expressing the penalization in terms of the penalty matrix \mathbf{Q}_{lm} as $\gamma_{lm}^h \boldsymbol{\kappa}_{lm}' \mathbf{Q}_{lm} \boldsymbol{\kappa}_{lm}$ lets us interpret it as resulting from a smoothing prior $\boldsymbol{\kappa}_{lm} \sim N(\mathbf{0}, \mathbf{Q}_{lm}^- / \gamma_{lm}^h)$. Decomposing $\tilde{\mathbf{W}}$ into a part \mathbf{W}_{lm} in the nullspace of \mathbf{Q}_{lm} and a part \mathbf{R}_{lm} in the range space of \mathbf{Q}_{lm} , we have

$$\mathbf{h}_{lm} = \mathbf{W}_{lm} \boldsymbol{\gamma}_{lm} + \mathbf{R}_{lm} \boldsymbol{\eta}_{lm}^h, \quad (12)$$

where $\boldsymbol{\gamma}_{lm}$ are fixed effects and $\boldsymbol{\eta}_{lm}^h \sim N(\mathbf{0}, \mathbf{I} / \gamma_{lm}^h)$ are random effects. Now repeat this eigendecomposition for all $l = 2, \dots, L$ and $m = 1, \dots, M_l$, and define the matrix

$$\mathbf{W} = \begin{bmatrix} \mathbf{W}_{21} & \dots & \mathbf{W}_{2,M_2} & \dots & \dots & \mathbf{W}_{L,1} & \dots & \mathbf{W}_{L,M_L} \end{bmatrix}$$

with j th row \mathbf{w}_j . Also define the matrix of fixed effects

$$\boldsymbol{\Gamma} = \begin{bmatrix} \gamma'_{21} & \dots & \gamma'_{2,M_2} & \mathbf{0} & \dots & & \mathbf{0} \\ \mathbf{0} & \dots & \mathbf{0} & \gamma'_{31} & \dots & \gamma'_{3,M_3} & \mathbf{0} & \vdots \\ \vdots & & & & & & \ddots & \mathbf{0} \\ \mathbf{0} & \dots & & & & & \mathbf{0} & \gamma'_{L,1} & \dots & \gamma'_{L,M_L} \end{bmatrix} \quad (13)$$

which has $L - 1$ rows and $\sum_{l=2}^L \sum_{m=1}^{M_l} \text{ncol}(\mathbf{W}_{lm})$ columns. Similarly define the matrix

$$\mathbf{Z}^h = \begin{bmatrix} \mathbf{R}_{21} & \dots & \mathbf{R}_{2,M_2} & \dots & \dots & \mathbf{R}_{L1} & \dots & \mathbf{R}_{L,M_L} \end{bmatrix} \quad (14)$$

whose j th row is \mathbf{z}_j^h and the random effects

$$\boldsymbol{\eta}^h = \left(\boldsymbol{\eta}_{21}^{h'} \quad \dots \quad \boldsymbol{\eta}_{2,M_2}^{h'} \quad \dots \quad \boldsymbol{\eta}_{L1}^{h'} \quad \dots \quad \boldsymbol{\eta}_{L,M_L}^{h'} \right)', \quad (15)$$

and let M_{L+1}^h denote the number of elements in $\boldsymbol{\eta}^h$.

2.2.3 GLLAMM Formulation

We now derive a GLLAMM formulation of the GALAMM defined by (4) and (6). Start by combining (11) and (15) into the vector of latent variables varying at level $L + 1$ as

$$\boldsymbol{\eta}^{(L+1)} = (\boldsymbol{\eta}^f, \boldsymbol{\eta}^h)'. \quad (16)$$

Let $M_{L+1} = M_{L+1}^f + M_{L+1}^h$, and define the measurement model and structural model by

$$\nu_i = \mathbf{x}_i' \boldsymbol{\beta} + \sum_{l=1}^{L+1} \sum_{m=1}^{M_l} \eta_m^{(l)} \mathbf{z}_{mi}^{(l)'} \boldsymbol{\lambda}_m^{(l)} \quad (17)$$

$$\boldsymbol{\eta}_j = \mathbf{B} \boldsymbol{\eta}_j + \boldsymbol{\Gamma} \mathbf{w}_j + \boldsymbol{\zeta}_j, \quad (18)$$

Letting $\pi_1(n)$ be a function which returns the indices (l, m) of the smooth function $h_{lm}(\cdot)$ for which $\eta_n^{(L+1)}$ is a random effect according to (12) and (16), we impose the constraints

$$\boldsymbol{\lambda}_n^{(L+1)} = \begin{cases} 1 & \text{for } n = 1, \dots, M_{L+1}^f \\ \boldsymbol{\lambda}_m^{(l)} & \text{for } (l, m) = \pi_1(n), n = M_{L+1}^f + 1, \dots, M_{L+1}, \end{cases} \quad (19)$$

and

$$\mathbf{z}_{ni}^{(L+1)} = \begin{cases} z_{ni}^f & \text{for } n = 1, \dots, M_{L+1}^f \\ z_{nj}^h \mathbf{z}_{mi}^{(l)} & \text{for } (l, m) = \pi_1(n), n = M_{L+1}^f + 1, \dots, M_{L+1}, \end{cases} \quad (20)$$

where z_{ni}^f is the element in the i th row and n th column of \mathbf{Z}^f defined in (10) and z_{nj}^h is the element in the j th row and n th column of \mathbf{Z}^h defined in (14), with j indexing the level-2 unit to which the i th level-1 unit belongs. The first line in constraint (19) ensures that the random effects at level $L + 1$ corresponding

to smooth terms in the measurement model receive a factor loading equal to 1 and hence can be placed in the structural model, and the first line in (20) makes sure that the corresponding explanatory variable is defined correctly. The second lines in constraints (19) and (20) ensure that random effects varying at level $L + 1$ corresponding to smooth functions predicting the m th latent variables at level l are multiplied by the same factor loading and covariate as the fixed effect part of their smooth function. In (17), $\mathbf{x}_i' \boldsymbol{\beta}$ is the fixed effect part of the smooth functions $f_s(\cdot)$, and in (18) the latent variables varying at level $L + 1$ are defined by $\boldsymbol{\eta}_j^{(L+1)} = \boldsymbol{\zeta}_j^{(L+1)} \sim N\{\mathbf{0}, \boldsymbol{\Psi}^{(L+1)}\}$, where $\boldsymbol{\Psi}^{(L+1)}$ is a diagonal matrix with diagonal elements $(\gamma_1^f, \dots, \gamma_S^f, \gamma_{21}^h, \dots, \gamma_{2,M_2}^h, \dots, \gamma_{L,M_L}^h)'$. The matrix \mathbf{F} in (18) contains the unpenalized parameters of the smooth terms in the structural model, as defined by (13).

2.3 Reduced Form

Since \mathbf{B} is strictly upper diagonal, $\mathbf{I} - \mathbf{B}$ is invertible and we can solve the structural model (6) for $\boldsymbol{\eta}_j$ to get

$$\boldsymbol{\eta}_j = (\mathbf{I} - \mathbf{B})^{-1} \{\mathbf{h}(\mathbf{w}_j) + \boldsymbol{\zeta}_j\} = \mathbf{C} \{\mathbf{h}(\mathbf{w}_j) + \boldsymbol{\zeta}_j\}, \quad (21)$$

where we define the $M \times M$ matrix $\mathbf{C} = (\mathbf{I} - \mathbf{B})^{-1}$ and let $c_{i,j}$ denote the element in its i th row and j th column. Let $\pi_2(l, m)$ denote a function which takes as arguments the level l and index m of a latent variable $\eta_m^{(l)}$, and returns its position in the full latent variable vector $\boldsymbol{\eta}$ defined in (1). With properly permuted indices, $\pi_2(l, m) = m + \sum_{\tilde{l}=1}^{l-1} M_{\tilde{l}}$. It follows from (21) that the scalar form of the structural model (6) is

$$\eta_{mj}^{(l)} = \sum_{\tilde{l}=2}^L \sum_{\tilde{m}=1}^{M_{\tilde{l}}} c_{\pi_2(l,m), \pi_2(\tilde{l}, \tilde{m})} \left[h_{\tilde{l}\tilde{m}} \left\{ \mathbf{w}_j^{(\tilde{l}+)} \right\} + \zeta_{\tilde{m}j}^{(\tilde{l})} \right], \quad l = 2, \dots, L, \quad m = 1, \dots, M_l, \quad (22)$$

where we now use index j to make it explicit that $\eta_{mj}^{(l)}$ is the value of the m th latent variable varying at level l for the j th level-2 unit, and similarly for the disturbance term $\zeta_{mj}^{(l)}$. Plugging (22) into the measurement model (4) gives the reduced form

$$\nu_i = \sum_{s=1}^S f_s(\mathbf{x}_i) + \sum_{l=2}^L \sum_{m=1}^{M_l} \left\{ \mathbf{z}_{mi}^{(l)'} \boldsymbol{\lambda}_m^{(l)} \right\} \sum_{\tilde{l}=2}^L \sum_{\tilde{m}=1}^{M_{\tilde{l}}} c_{\pi_2(l,m), \pi_2(\tilde{l}, \tilde{m})} \left[h_{\tilde{l}\tilde{m}} \left\{ \mathbf{w}_j^{(\tilde{l}+)} \right\} + \zeta_{\tilde{m}j}^{(\tilde{l})} \right], \quad (23)$$

where the parameters to be estimated are $\boldsymbol{\lambda}_m^{(l)}$, $c_{m,\tilde{m}}$, and the weights ω_{ks} in $f_s(\mathbf{x}_i)$ and κ_{klm} in $h_{lm}\{\mathbf{w}_j^{(l)}\}$. The regression coefficients between latent variables can be converted back to their original form from the estimates of $c_{m,\tilde{m}}$ through the transformation $\mathbf{B} = \mathbf{I} - \mathbf{C}^{-1}$.

In terms of the mixed model formulation (17)-(18) we can derive the equivalent reduced form

$$\nu_i = \mathbf{x}_i' \boldsymbol{\beta} + \sum_{\tilde{l}=2}^{L+1} \sum_{\tilde{m}=1}^{M_{\tilde{l}}} \sum_{l=2}^{L+1} \sum_{m=1}^{M_l} \left\{ \mathbf{z}_{mi}^{(l)'} \boldsymbol{\lambda}_m^{(l)} \right\} c_{\pi(l,m),\pi(\tilde{l},\tilde{m})} \left\{ \boldsymbol{\Gamma}_{\pi_2(l,m),\cdot} \mathbf{w}_j + \zeta_{\tilde{m}j}^{(\tilde{l})} \right\}, \quad (24)$$

where $\boldsymbol{\Gamma}_{j,\cdot}$ denotes the j th row of $\boldsymbol{\Gamma}$ and hence $\boldsymbol{\Gamma}_{\pi_2(l,m),\cdot} \mathbf{w}_j$ is a scalar.

2.4 Profile Likelihood Estimation

The reduced form (24) is a nonlinear mixed model containing products of fixed effects as well as products between fixed and random effects, and the linear predictor is in general linked to the observed outcome with a nonlinear link function. We now describe an extension of the profile likelihood approach proposed by Jeon and Rabe-Hesketh (2012) for maximum likelihood estimation of GALAMMs defined by (4) and (6). The algorithm combines existing GAMM software with a general purpose optimization routine, thus requiring limited additional programming. Since the conversion to mixed model representation is performed automatically by the GAMM software, we derive the method from the reduced form (23) rather than the mixed model version (24).

Assume estimates $\hat{\boldsymbol{\lambda}}_m^{(l)}$ and $\hat{c}_{\pi(l,m),\pi(\tilde{l},\tilde{m})}$ are available, and fix $\boldsymbol{\lambda}_m^{(l)}$ and $c_{\pi(l,m),\pi(\tilde{l},\tilde{m})}$ in (23) to these values to get

$$\nu_i = \sum_{s=1}^S f_s(\mathbf{x}_i) + \sum_{\tilde{l}=2}^L \sum_{\tilde{m}=1}^{M_{\tilde{l}}} \sum_{l=2}^L \sum_{m=1}^{M_l} \left\{ \mathbf{z}_{mi}^{(l)'} \hat{\boldsymbol{\lambda}}_m^{(l)} \right\} \hat{c}_{\pi(l,m),\pi(\tilde{l},\tilde{m})} \left[h_{\tilde{l}\tilde{m}} \left\{ \mathbf{w}_j^{(\tilde{l}+)} \right\} + \zeta_{\tilde{m}j}^{(\tilde{l})} \right], \quad (25)$$

which can be recognized as a GAMM. The first term on the right-hand side contains S smooth terms $f_s(\mathbf{x}_i)$. Expanding the square brackets, the second term contains M varying-coefficient terms (Hastie and Tibshirani, 1993) of the form

$$h_{\tilde{l}\tilde{m}} \left\{ \mathbf{w}_j^{(\tilde{l}+)} \right\} \sum_{l=2}^L \sum_{m=1}^{M_l} \left\{ \mathbf{z}_{mi}^{(l)'} \hat{\boldsymbol{\lambda}}_m^{(l)} \right\} \hat{c}_{\pi(l,m),\pi(\tilde{l},\tilde{m})}, \quad \tilde{l} = 2, \dots, L, \quad \tilde{m} = 1, \dots, M_{\tilde{l}}.$$

It may help intuition to consider the case with no regressions between latent variables, for which $\mathbf{C} = (\mathbf{I} - \mathbf{0})^{-1} = \mathbf{I}$ and the varying-coefficient terms simplify to

$$\mathbf{z}_{mi}^{(l)'} \hat{\boldsymbol{\lambda}}_m^{(l)} h_{lm} \left\{ \mathbf{w}_j^{(l+)} \right\}, \quad l = 2, \dots, L, \quad m = 1, \dots, M_l,$$

with $h_{lm}(\cdot)$ now a smoothly varying regression coefficient for $\mathbf{z}_{mi}^{(l)'} \hat{\boldsymbol{\lambda}}_m^{(l)}$. The last term inside the square brackets in (25) contains M random effects.

Let Θ denote the set of all parameters of the GALAMM in mixed model formulation (17)-(18), including

random coefficients varying at level $L + 1$. Defining $\mathbf{\Lambda}^{(l)} = [\boldsymbol{\lambda}_1^{(l)} \dots \boldsymbol{\lambda}_{M_l}^{(l)}]$ and $\mathbf{\Lambda} = [\mathbf{\Lambda}^{(2)} \dots \mathbf{\Lambda}^{(L)}]$, we divide Θ into $\Theta_1 = \{\mathbf{\Lambda}, \mathbf{B}\}$ and Θ_2 containing all remaining parameters. We similarly define the likelihood as a function of these two parameter sets $L(\Theta) = L(\Theta_1, \Theta_2)$. Let

$$\hat{\Theta}_2(\Theta_1) = \operatorname{argmax}_{\Theta_2} L(\Theta_1, \Theta_2), \quad (26)$$

define the maximum likelihood estimates of the parameters in Θ_2 as a function of the parameters in Θ_1 , and define the profile likelihood

$$L(\Theta_1) = \max_{\Theta_2} L(\Theta_1, \Theta_2) = L\left\{\Theta_1, \hat{\Theta}_2(\Theta_1)\right\}. \quad (27)$$

Equations (26) and (27) can be iterated to obtain the maximum likelihood estimates of Θ . In the inner step, (26) is computed at Θ_1 by solving the GAMM (25) after plugging in values of $\hat{\boldsymbol{\lambda}}_m$ and $\hat{c}_{\pi(l,m), \pi(\tilde{l}, \tilde{m})}$ from Θ_1 . In the outer step, $L(\Theta_1)$ is maximized with respect to Θ_1 . Convergence is achieved when changing Θ_1 along any of its dimensions no longer leads to an increase in $L(\Theta_1)$.

For fixed values of $\hat{\Theta}_1$, R packages 'mgcv' (Wood, 2017) and 'gamm4' (Wood and Scheipl, 2020) solve (26) efficiently. While 'gamm4' uses 'lme4' (Bates et al., 2015) to solve the underlying GLMM with a full Laplace approximation, the `gamm` function in 'mgcv' uses the 'nlme' package (Pinheiro et al., 2020) for Gaussian models with unit link and `glmmPQL` from the 'MASS' package (Venables and Ripley, 2002) otherwise. As the latter uses penalized quasilielihood (Breslow and Clayton, 1993; Schall, 1991), maximum likelihood estimates are not obtained, and hence 'gamm4' will typically be preferable in the generalized case. The profile likelihood (27) can be maximized with a general purpose optimization routine, as available in the base R `optim()` function, using the log likelihood of the GAMM (26) as objective function. In our experiments, both the Nelder-Mead algorithm (Nelder and Mead, 1965) and the limited-memory Broyden-Fletcher-Goldfarb-Shanno algorithm with box constraints (L-BFGS-B) (Byrd et al., 1995) have achieved stable and good performance, with the latter typically being faster. While Nelder-Mead is derivative free, L-BFGS-B also uses the gradient of the log likelihood with respect to Θ_1 when maximizing (27), which can be obtained using finite differences.

2.5 Standard Errors

Let $\hat{\Theta} = (\hat{\Theta}_1, \hat{\Theta}_2)$ denote the estimates obtained by profile likelihood estimation. The Fisher information matrix $\mathbf{I}(\hat{\Theta}_1, \hat{\Theta}_2)$ and its inverse can be defined by

$$\mathbf{I}(\hat{\Theta}_1, \hat{\Theta}_2) = \begin{bmatrix} \mathbf{I}_{(\hat{\Theta}_1, \hat{\Theta}_1)} & \mathbf{I}_{(\hat{\Theta}_1, \hat{\Theta}_2)} \\ \mathbf{I}_{(\hat{\Theta}_2, \hat{\Theta}_1)} & \mathbf{I}_{(\hat{\Theta}_2, \hat{\Theta}_2)} \end{bmatrix} \text{ and } \mathbf{I}^{-1}(\hat{\Theta}_1, \hat{\Theta}_2) = \begin{bmatrix} \mathbf{C}_{(\hat{\Theta}_1, \hat{\Theta}_1)} & \mathbf{C}_{(\hat{\Theta}_1, \hat{\Theta}_2)} \\ \mathbf{C}_{(\hat{\Theta}_2, \hat{\Theta}_1)} & \mathbf{C}_{(\hat{\Theta}_2, \hat{\Theta}_2)} \end{bmatrix}.$$

The block $\mathbf{C}_{(\hat{\Theta}_1, \hat{\Theta}_1)}$ is the covariance matrix of $\hat{\Theta}_1$ taking uncertainty in $\hat{\Theta}_2$ into account, and is readily obtained from the profile likelihood algorithm (26)–(27) as minus the inverse of the Hessian evaluated at the final estimates of $\hat{\Theta}_1$ (Jeon and Rabe-Hesketh, 2012). The covariance matrix obtained when solving (26) corresponds to $\mathbf{I}_{(\hat{\Theta}_2, \hat{\Theta}_2)}^{-1}$ and does not take uncertainty in $\hat{\Theta}_1$ into account. Following Parke (1986), Jeon and Rabe-Hesketh (2012) defined the asymptotic covariance matrix of $\hat{\Theta}_2$ as

$$\text{Cov}(\hat{\Theta}_2, \hat{\Theta}_2) = \mathbf{I}_{(\hat{\Theta}_2, \hat{\Theta}_2)}^{-1} + \left[\frac{\partial \hat{\Theta}_2(\Theta_1)}{\partial \Theta_1} \bigg|_{\Theta_1 = \hat{\Theta}_1} \right] \mathbf{C}_{(\hat{\Theta}_1, \hat{\Theta}_1)} \left[\frac{\partial \hat{\Theta}_2(\Theta_1)}{\partial \Theta_1} \bigg|_{\Theta_1 = \hat{\Theta}_1} \right]'. \quad (28)$$

It also follows from Parke (1986) that

$$\text{Cov}(\hat{\Theta}_1, \hat{\Theta}_2) = \text{Cov}(\hat{\Theta}_2, \hat{\Theta}_1)' = \mathbf{C}_{(\hat{\Theta}_1, \hat{\Theta}_1)} \left[\frac{\partial \hat{\Theta}_2(\Theta_1)}{\partial \Theta_1} \bigg|_{\Theta_1 = \hat{\Theta}_1} \right]', \quad (29)$$

which lets us define the full asymptotic covariance matrix of Θ as

$$\text{Cov}(\hat{\Theta}) = \begin{bmatrix} \mathbf{C}_{(\hat{\Theta}_1, \hat{\Theta}_1)} & \text{Cov}(\hat{\Theta}_1, \hat{\Theta}_2) \\ \text{Cov}(\hat{\Theta}_2, \hat{\Theta}_1) & \text{Cov}(\hat{\Theta}_2, \hat{\Theta}_2) \end{bmatrix}. \quad (30)$$

With a one-sided finite difference scheme, the Jacobian $\partial \hat{\Theta}_2(\Theta_1)/\partial \Theta_1$ in (28) and (29) requires computing the GAMM (26) once for each element of Θ_1 , and since the derivative with respect to each component of Θ_1 can be computed independently, we recognize this as a perfectly parallel problem.

Asymptotic standard errors of parametric components are obtained from the corresponding elements of $\text{Cov}(\hat{\Theta})$. Standard errors for smooth terms, or for prediction in general, requires consideration of multiple elements of $\text{Cov}(\hat{\Theta})$. For example, consider the function $f_s(\mathbf{x}_i)$ in equation (5), define $\tilde{\mathbf{X}}_s$ as in (8), let $\hat{\omega}_s \subset \hat{\Theta}_2$ be the vector of estimated weights, and $\text{Cov}(\hat{\omega}_s)$ a submatrix of $\text{Cov}(\hat{\Theta})$ restricted to the columns corresponding to $\hat{\omega}_s$. The estimate of this smooth term equals $\hat{\mathbf{f}}_s = \tilde{\mathbf{X}}_s \hat{\omega}_s$, and defining $\mathbf{v}_s = \text{diag}(\tilde{\mathbf{X}}_s \text{Cov}(\hat{\omega}_s) \tilde{\mathbf{X}}_s')$, the standard error at the i th evaluation point is $\sqrt{v_{si}}$, the i th element of \mathbf{v}_s . Approximate pointwise confi-

dence intervals over the evaluation points are given by $f_{si} \pm z_{\alpha/2} \sqrt{v_{si}}$, where $z_{\alpha/2}$ is the $\alpha/2$ quantile of the standard normal distribution (Wood, 2017, Chapter 6.10). Confidence intervals constructed this way have approximately $(1 - \alpha)100\%$ coverage averaged over the domain of the function (Marra and Wood, 2012). In contrast, simultaneous confidence intervals which cover the function over its whole domain with probability $(1 - \alpha)100\%$ require a critical value $\tilde{z}_{\alpha/2} \geq z_{\alpha/2}$. An estimate of $\tilde{z}_{\alpha/2}$ can be obtained by sampling from the empirical Bayes posterior distribution of $f_s(\cdot)$, and finding the quantile for which $(1 - \alpha)100\%$ of the sampled curves are completely confined within $f_{si} \pm \tilde{z}_{\alpha/2} \sqrt{v_{si}}$ (Ruppert et al., 2003, Chapter 6.5).

3 Applications and Simulation Experiments

We now present three example applications, each followed by a simulation study in which the data structure and model parameters closely mimicked the real data. All analyses were done in R 4.0.0 (R Core Team, 2020). In addition to the packages cited in the text, 'future' (Bengtsson, 2021) was used for parallel computation and the 'tidyverse' (?) for data processing and visualization.

3.1 Latent Response Models

3.1.1 Lifespan Trajectory of Episodic Memory

The California verbal learning test (CVLT) (Delis et al., 2000) is a widely used test of episodic memory. During the test, the experimenter reads a list of 16 words aloud, and subsequently the participant is asked to repeat the words. This procedure is repeated in five trials, and we treat the number of correct responses in each trial as level-1 units. Our dataset consisted of CVLT scores from 3470 observations of 1850 healthy participants between 6 and 93 years of age, from the Center for Lifespan Changes in Brain and Cognition (LCBC) (Fjell et al., 2018; Walhovd et al., 2016). Each participant completed the test between 1 and 6 times, and the time interval between two consecutive measurements varied between 5 weeks and 9.7 years, with mean interval 2.4 years. We defined the trials as level-1 units, so each timepoint for a given participant was a level-2 unit. As all participants had completed the full CVLT at each timepoint, each level-2 unit contained five level-1 units. The level-3 units were individual participants, containing between 1 and 6 level-2 units. Figure 1 shows that the number of words recalled varied nonlinearly across the lifespan, with a rapid increase during childhood, stability during adulthood, and decrease in old age. The participants recalled a larger number of words in the later trials, illustrating a within-timepoint learning effect. Ceiling effects are also apparent in later trials, as a large number of participants remembered all 16 words.

Assuming that the number of words recalled are noisy measurements of the participants' episodic memory,

our goal was to estimate how episodic memory varies with age. We defined a three-level GALAMM with binomially distributed level-1 responses $y_i \in \{0, \dots, 16\}$, using a logit link $\nu_i = g(\mu_i) = \log\{\mu_i/(1 - \mu_i)\}$ where μ_i is the expected proportion of successes. In terms of the exponential family (3), $\theta_i = g(\mu_i) = \nu_i$, $b(\theta_i) = \log\{1 + \exp(\theta_i)\}$, and $\phi = 1/16$, which simplifies to $\Pr(y_i|\mu_i) \propto \mu_i^{y_i} (1 - \mu_i)^{16-y_i}$. The measurement model and structural model took the form

$$\nu_i = \mathbf{d}'_{ti}\boldsymbol{\beta}_t + d_{ri}\beta_r + \mathbf{d}'_{ti}\boldsymbol{\lambda} \sum_{l=2}^3 \eta^{(l)} \quad (31)$$

$$\boldsymbol{\eta}_j = \begin{bmatrix} \eta_{jk}^{(2)} \\ \eta_k^{(3)} \end{bmatrix} = \begin{bmatrix} h(w_{jk}) \\ 0 \end{bmatrix} + \begin{bmatrix} \zeta_{jk}^{(2)} \\ \zeta_k^{(3)} \end{bmatrix}, \quad (32)$$

where unnecessary subscripts and superscripts are omitted. \mathbf{d}_{ti} is an indicator vector whose k th element equals one if the i th level-1 unit is a measurement of CVLT trial k and zero otherwise, and $\boldsymbol{\beta}_t = (\beta_{t1}, \dots, \beta_{t5})'$ is a vector of item effects. Retest effects, which can be defined as the marginal effect of having taken the CVLT previously (Woods et al., 2006), were accounted for by the variable $d_{ri} \in \{0, 1\}$ indicating whether the participant had taken the test previously at the given timepoint. The latent episodic memory $\eta_{jk}^{(2)}$ at timepoint j of participant k consists of a systematic component $h(w_{jk})$, which is a smooth function of age w_{jk} , and a random intercept $\zeta_{jk}^{(2)}$ varying between timepoints of a given participant. The smooth function was specified following (7), $h(w_{jk}) = \sum_{k=1}^D \kappa_k d(w_{jk})$ with $D = 15$ cubic regression splines and squared second derivative penalization. The latent variable $\eta_k^{(3)} = \zeta_k^{(3)}$ is a random intercept varying between participants. The random intercepts at each level were assumed normally distributed with mean zero, i.e., $\boldsymbol{\zeta} \sim N(\mathbf{0}, \boldsymbol{\Psi})$ where $\boldsymbol{\Psi} = \text{diag}(\psi^{(2)}, \psi^{(3)})$. In the measurement model (31) we have implicitly introduced the constraints $\mathbf{z}_i^{(2)} = \mathbf{z}_i^{(3)} = \mathbf{d}_{ti}$ and $\boldsymbol{\lambda}^{(2)} = \boldsymbol{\lambda}^{(3)} = \boldsymbol{\lambda}$, ensuring that $\eta_k^{(3)}$ can be interpreted as a random intercept for the latent level $\eta_{jk}^{(2)}$ (Rabe-Hesketh et al., 2004a, pp. 182–183). In the factor loadings $\boldsymbol{\lambda} = (\lambda_1, \dots, \lambda_5)'$, the constraint $\lambda_1 = 1$ was imposed for identifiability. Enforcing a point constraint $h(0) = 0$ on the smooth term will typically lead to too wide confidence intervals (Wood, 2017, Ch. 5.4.1), so instead $h(w_{jk})$ was freely estimated. It follows that the intercept for a given item $k \in \{1, \dots, 5\}$ equals $\beta_{tk} + \lambda_k h(0)$, where we constrained $\beta_{t1} = 0$ for identifiability.

Plugging (32) into (31) gives the reduced form

$$\nu_i = \mathbf{d}'_{ti}\boldsymbol{\beta}_t + d_{ri}\beta_r + h(w_{jk}) \mathbf{d}'_{ti}\boldsymbol{\lambda} + \zeta_{jk}^{(2)} \mathbf{d}'_{ti}\boldsymbol{\lambda} + \zeta_k^{(3)} \mathbf{d}'_{ti}\boldsymbol{\lambda}, \quad (33)$$

and inserting estimates $\hat{\boldsymbol{\lambda}}$, (33) is recognized as a GAMM with parametric terms $\mathbf{d}'_{ti}\boldsymbol{\beta}_t + d_{ri}\beta_r$, varying-coefficient term $h(w_{jk}) \mathbf{d}'_{ti}\hat{\boldsymbol{\lambda}}$, and random effects $\zeta_{jk}^{(2)}$ and $\zeta_k^{(3)}$ of $\mathbf{d}'_{ti}\hat{\boldsymbol{\lambda}}$. Defining $\Theta_1 = \{\boldsymbol{\lambda}\}$ and $\Theta_2 = \{\boldsymbol{\omega}, \boldsymbol{\kappa}, \boldsymbol{\Psi}\}$,

this representation was used to solve (26) in the profile likelihood algorithm using 'gamm4' (Wood and Scheipl, 2020), yielding estimates $\hat{\Theta}_2 = \{\hat{\omega}, \hat{\kappa}, \hat{\Psi}\}$ as a function of Θ_1 . To speed up computation, fixed effects and variance components from the previous step were used as starting values when computing (26). Estimates of $\hat{\Theta}_1 = \{\hat{\lambda}\}$ were computed by optimizing (27) with the L-BFGS-B algorithm (Byrd et al., 1995) using the base R function `optim()` and standard errors were computed following Section 2.5, using the R package 'numDeriv' (Gilbert and Varadhan, 2019) for calculation of Jacobians with a forward difference scheme. The full model estimation took about five hours, whereas using the Nelder-Mead algorithm (Nelder and Mead, 1965) instead required about 10 hours. Very similar estimates were obtained with thin-plate regression splines (Wood, 2003) and with $D = 30$ cubic regression splines.

Estimates of regression coefficients are shown in Table 1. The item effects increase with trial number, reflecting that participants on average achieve higher scores in later trials, and for several items the asymptotic standard errors computed with (28) were substantially higher than the uncorrected standard errors. From the estimated retest effect and its standard error we find that the odds ratio for correctly recalling a word when having taken the test previously compared to not having taken the test previously is $\exp(\beta_r) = 1.16$. The variance components were estimated to $\sqrt{\hat{\psi}^{(2)}} = 0.26$ and $\sqrt{\hat{\psi}^{(2)}} = 0.28$, indicating that conditional on the explanatory variables, a single participant's variation between timepoints is of comparable magnitude to the variation between participants.

Item characteristic curves show the probability of a correct response in trial k as a function of the latent level, $f_k\{\eta^{(2)}\} = (1 + \exp[-\{\beta_{tk} + \lambda_k\eta^{(2)}\}])^{-1}$ (Skrondal and Rabe-Hesketh, 2004, Ch. 3.3.4), and are shown in Figure 2 (left) together with estimates and standard errors of factor loadings. The curve for trial 1 equals $f_1\{\eta^{(2)}\} = [1 + \exp\{-\eta^{(2)}\}]^{-1}$ due to the identifiability restrictions imposed, and all other curves are defined relative to this one. The items' ability to discriminate between high and low levels of episodic memory increases from trial 1 to trial 5, and the increasingly positive item effects for trials 2-5 imply that the probability of correct response at the average level of episodic memory gets increasingly close to 1. The estimated lifespan trajectory of episodic memory is shown in Figure 2 (right). It shows a steep increase during childhood until the age of around 18, followed by a period of stability during young adulthood, slow decline between the age of 35 and 75, and finally a steep decrease after the age of 75. Simultaneous confidence intervals required a critical value 3.06 at 95% confidence level, and are shown in light gray in Figure 2 (right).

The timing of age-related decline in cognitive function has received much focus, with cross-sectional studies indicating that the decline starts around the age of 20 (Salthouse, 2009) and longitudinal studies showing a stable level until the age of 60 (Rönnlund et al., 2005). Debate has concerned the relative magnitude of cohort effect bias in cross-sectional studies versus retest effect bias in longitudinal studies (Nilsson et al., 2009; Raz and Lindenberger, 2011; Salthouse, 2009; Schaie, 2009). When retest effects are

properly accounted for in longitudinal studies, the difference between the approaches is typically reduced (Tucker-Drob et al., 2019), suggesting that retest effects are larger than cohort effects. The trajectory in Figure 2 (right) shows some agreement with Salthouse (2009), but all the aforementioned studies used restrictive parametric models and are hence not directly comparable. The GALAMM-based model presented in this section offers the opportunity for more accurate estimation of lifespan cognitive development.

3.1.2 Simulation Experiments

Simulation experiments were conducted based on the model estimated in the last section. The Laplace approximation used to fit the GAMM in equation (26) is asymptotically consistent (Vonesh, 1996), as is the overall profile likelihood algorithm (Parke, 1986), but it is of interest to investigate their finite sample properties. To this end, we simulated 500 random datasets with 200, 500, and 1000 participants each. Probability distributions for age at measurement, time interval between measurements, and number of timepoints per participant were estimated from the LCBC data, and new values randomly sampled from these distributions. Since the participants are level-3 units, with an average number of timepoints equal to 1.88 and five CVLT items observed at each timepoint, the expected total number of level-1 units with the three different samples sizes were 940, 4700, and 9400. For detailed description of the simulation distributions, see Supplementary Section S1.2. The model set-up was identical to Section 3.1.1.

Figure 3 shows simulation results for parametric terms, with relative bias between an estimate $\hat{\beta}$ and the true value β defined as $(\hat{\beta} - \beta)/\beta$. Both the item effects and the retest effect showed a positive bias with 200 participants. For the item effects, this bias was considerably reduced with 500 participants, and close to zero with 1000 participants. For the retest effect, on the other hand, the bias was still around 2.5% with 1000 participants, down from around 6% with 200 participants. For the factor loadings, the bias was moderate at all sample sizes. Coverage of 95% confidence intervals for all parameter was close to nominal at all sample sizes. Confidence intervals for coverage probabilities here and in the rest of the paper were computed using Wilson’s score interval with continuity correction. Similar low bias was observed for estimated variance components (Supplementary Figure S1). As shown in the third column of Figure 3, the mean square error (MSE) of all parameters decreased consistently with sample size. The ratio of MSE with 1000 participants to MSE with 200 participants ranged from 0.16 to 0.20, which is close to the expected value $200/1000 = 0.20$ under root- n consistency.

Figure 4 (left) shows that across-the-function coverage of pointwise confidence intervals are close to nominal for all sample sizes. The simultaneous confidence intervals had slightly below nominal coverage, around 93%. Hypothesizing that a larger basis would reduce bias with large sample sizes (e.g., Hall and Opsomer (2005)) and hence increase interval coverage, we performed an additional set of simulations using

30 cubic regression splines with 1000 participants. However, the results showed essentially no difference from using a basis of size 15. The center plot in Figure 4 shows that pointwise confidence intervals achieve close to nominal coverage by having above nominal coverage over parts of the range and below nominal coverage over other parts, as also demonstrated by Ruppert and Carroll (2000). Comparison with the true curve in Figure 2 suggests that the coverage is low in regions where the smooth curve changes rapidly, in childhood and in old age, and the coverage is high when the curve is close to linear, during most of adulthood. Squared bias and variance were computed separately at each age across Monte Carlo estimates, and then averaged across the full age range, and are shown in the right plot in Figure 4, together with their sum (MSE). Squared bias amounted to 20% of the MSE at 200 participants, 21.8% at 500 participants, and 18.6% at 1000 participants, suggesting that the proportion of bias is fairly constant within this range of sample sizes.

3.2 Factor-by-Curve Interaction Model with Latent Responses

3.2.1 Joint Modeling of Episodic and Working Memory

Episodic memory, considered in Section 3.1.1, involves recollection of specific events. Working memory, on the other hand, involves the ability to hold information temporarily. Dating back at least to Spearman (1904), individual abilities in cognitive domains are known to be correlated, and we will here demonstrate how GALAMMs with multiple smooth terms can be used to model lifespan trajectories of cognitive abilities in multiple domains. In addition to the CVLT measurements described in the previous section, the data contained measurements of working memory assessed by digit span tests. In a digit span test, a sequence of numbers of increasing length is read out loud, and the final score is defined as the length of the longest list of numbers the participant is able to immediately repeat back (Blackburn and Benton, 1959). In an additional test, the participant is instead asked to repeat the list of numbers backwards. Both experiments are repeated up to a list of length 16, which is the maximum possible score. The total sample consisted of 3763 timepoints for 1924 individuals, of which 1781 had both CVLT and digit span scores in at least one timepoint. The number of level-1 units was 24244. Supplementary Figure S5 shows item responses to the digit span tests.

We modeled the maximum length of the lists recalled in the digit span forward and backward tests as binomially distributed variables with 16 trials, and could thus use a logistic link for both the digit span items and the CVLT items. Extending model (31)-(32) we defined

$$\nu_i = \mathbf{d}'_{ti}\boldsymbol{\beta}_t + \mathbf{d}'_{ri}\boldsymbol{\beta}_r + \sum_{l=2}^3 \sum_{m=1}^2 \mathbf{d}'_{ti}\boldsymbol{\lambda}_m\eta_m^{(l)}, \quad (34)$$

$$\boldsymbol{\eta} = \begin{bmatrix} \eta_1^{(2)} \\ \eta_2^{(2)} \\ \eta_1^{(3)} \\ \eta_2^{(3)} \end{bmatrix} = \begin{bmatrix} h_1(w) \\ h_2(w) \\ 0 \\ 0 \end{bmatrix} + \begin{bmatrix} \zeta_1^{(2)} \\ \zeta_2^{(2)} \\ \zeta_1^{(3)} \\ \zeta_2^{(3)} \end{bmatrix}. \quad (35)$$

In the measurement model (34), $\mathbf{d}'_{it}\boldsymbol{\beta}_t$ contains item effects, now also including digit span forward and backward. We modeled the retest effects separately, such that \mathbf{d}_{ri} now is a vector of size 2, whose first element is an indicator for the event that the participant has taken the CVLT at a previous time, and whose second element is a similar indicator for the digit span test. It follows that $\boldsymbol{\beta}_r = (\beta_{r1}, \beta_{r2})'$ contains retest effects for the CVLT and digit span test, respectively. The first vector of factor loadings $\boldsymbol{\lambda}_1 = (\lambda_{11}, \dots, \lambda_{15})'$ is defined as in the previous section, while the second vector $\boldsymbol{\lambda}_2 = (\lambda_{21}, \lambda_{22})'$ contains loadings relating working memory to measured digit span. For identifiability, we set $\lambda_{11} = 1$ and $\lambda_{21} = 1$. In the structural model (35), $h_1(w)$ and $h_2(w)$ model episodic memory and working memory as smooth functions of age, each defined as the linear combination of ten cubic regression splines, with squared second derivative penalization. Since episodic and working memory are closely related, we defined these with factor-by-curve interaction models with a common smoothing parameter (Coull et al., 2001). In terms of the mixed model representation defined in equation (12), dropping unnecessary indices, these smooth functions have only a random part

$$h_m = \mathbf{R}_m \boldsymbol{\eta}_m = \eta_{m1} + w\eta_{m2} + \mathbf{R}_{m3} \boldsymbol{\eta}_{m3}, \quad m = 1, 2,$$

with $\eta_{m1} \sim N\{0, \psi_1^{(4)}\}$ a random intercept for the overall level, $\eta_{m2} \sim N\{0, \psi_2^{(4)}\}$ a random linear slope, and \mathbf{R}_{m3} a matrix in the range space of the squared second derivative smoothing penalty, with $\boldsymbol{\eta}_{m3} \sim N\{\mathbf{0}, \psi_3^{(4)} \mathbf{I}_8\}$ the corresponding random effect. The terms $\zeta_1^{(2)}$ and $\zeta_2^{(3)}$ in (35) are random intercepts for episodic and working memory, respectively, varying between timepoints for the same participant, while $\zeta_1^{(3)}$ and $\zeta_2^{(3)}$ are random effects varying between participants. Their covariance matrices were freely estimated. Since the structural model contained no constant fixed term, all seven items were explicitly represented in the item effect term $\mathbf{d}'_{it}\boldsymbol{\beta}_t$ in the measurement model.

Model estimation was performed as described for the CVLT model in Section 3.1.1, and took about two days. The correlation between level-3 random intercepts $\zeta_1^{(3)}$ and $\zeta_2^{(3)}$ was estimated to 0.41, indicating that conditional on age, there is a fairly strong positive correlation between individual levels of episodic and working memory. This is slightly below a recent meta analysis of adult samples by Tucker-Drob et al. (2019) who found a level communality of 0.56 across a large range of cognitive domains. Surprisingly, the correlation of level-2 intercepts was estimated to 1.0, which at face value indicates that a person's deviation

from her/his long-term level at any given day is identical across episodic and working memory. However, simulation experiments shown in Section 3.2.2 suggest that it is not possible to accurately estimate the level-2 correlation with the low number of timepoints per participant characteristic of these data, and we should hence not interpret it further.

Figure 5 (left) shows the estimated lifespan trajectories for episodic and working memory. We estimated the difference in age at maximum of the two curves by drawing 10000 random samples from the empirical Bayes posterior distributions of the spline weights, computing the trajectories on a dense grid between the age of 10 and 60, and recording the difference between the age at maximum working memory and the age at maximum episodic memory. Figure 5 (right) shows the posterior distribution of the difference, which has a mean of 7 years. A 95% highest posterior density interval indicated by the horizontal bar at the bottom of the plot, spans differences from -3.0 years to 16.7 years. It follows that we cannot conclude from these data whether working memory peaks at a higher age than episodic memory. The ceiling effects apparent in the CVLT (Figure 1, left) but not in the digit span test (Supplementary Figure S5) represent a potential confounding factor, as they may lead to a large number of participants achieving a maximum score before their maximum latent level is reached.

3.2.2 Simulation Experiments

Simulation experiments were performed with the goal of understanding the accuracy of the estimated correlations between latent variables at level 2 and level 3. Due to the high computational requirement, the factor loadings were fixed at their estimated values, such that only the GAMM part (26) of the profile likelihood algorithm had to be computed. The simulated data were close to the real data and model estimates, but with level-2 correlation set to 0.5 rather than the estimated 1.0, and level-3 correlation set at the estimate 0.41. Hypothesizing that correlations would be more accurately estimated with an increasing number of timepoints per individuals, we considered (1) the original setting in which 45.9% of the participants were measured at a single timepoint, (2) a setting in which all participants had at least two timepoints, and (3) a setting in which all participants had at least three timepoints. These cases were combined with (a) a setting in which the particular tests taken at each timepoint followed the original data, and (b) a setting in which each participant had completed both the CVLT and the digit span test at each timepoint. For each setting, 100 Monte Carlo samples were generated. Details are provided in Supplementary Section S2.2.

The results indicated that level-3 correlation was accurately estimated with minimal bias in all settings (Supplementary Figure S8), whereas level-2 correlation was highly inaccurate. In the simulation setting closest to the original data (1a), the estimated level-2 correlation varied between -1 and +1, with a peak at 1 (Supplementary Figure S7). Even with complete data and at least three timepoints per individual

(3a), the distribution varied between 0 and 1, with a peak at 1. Importantly, this inaccurate estimation of level-2 correlation did not show negative consequences for the other model parameters. Across-the-function coverage of pointwise confidence intervals for smooth terms were close to nominal (Supplementary Figure S6), and the root-mean-square error of the estimated smooth terms was not correlated with the estimated level-2 correlation (Supplementary Figure S9).

3.3 Latent Covariates

3.3.1 Socioeconomic Status and Hippocampus Volume

The association between socioeconomic status and brain development has been the subject of much research. It has been proposed that higher socioeconomic status during childhood protects against late-life dementia (Livingston et al., 2017), whereas a meta-analysis found that the associations between socioeconomic status and brain structure varied considerably between samples (Walhovd et al., 2020a). The hippocampus is a brain region which plays an important role in memory consolidation, and is one of the first regions to be damaged in Alzheimer’s disease (Dubois et al., 2016). Positive associations have been found between socioeconomic status and hippocampal volume in children (Hanson et al., 2011; Noble et al., 2012; Yu et al., 2018), and between childhood socioeconomic status and adult brain size (Staff et al., 2012). However, while hippocampal volume is known to be a nonlinear function of age, most studies investigating the association have used linear regression analyses. An exception is Nyberg et al. (2021), who used GAMMs to model the hippocampal trajectory, and found no relationship between longitudinal change in hippocampal volume and educational attainment in two large adult samples.

We here consider the association between hippocampal volume and socioeconomic status across the lifespan, still using data from the Center for Lifespan Changes in Brain and Cognition (Fjell et al., 2018; Walhovd et al., 2016). Hippocampal volumes were estimated with FreeSurfer 7 (Dale et al., 1999; Fischl et al., 2002; Reuter et al., 2012) from magnetic resonance images obtained at four different scanners, and are shown in Figure 6. In total, we had 4196 scans of 1886 participants aged between 4 and 93 years, with between 1 and 7 scans per participant. Our interest concerns how the lifespan trajectory of hippocampal volume depends on socioeconomic status. For participants below the age of twenty, we defined socioeconomic status based on their father’s and mother’s years of completed education and income, and for participants above the age of twenty we defined it based on their own education and income. As these variables were typically only measured at a single timepoint, they were considered time-independent. Of the 1886 participants with hippocampal volume measurements, either their own or at least one parent’s education level was available from 1681 participants, while the corresponding number for income was 538. All timepoints for the 205

participants with no measurement of socioeconomic status were also included in the analyses, yielding a total of 7130 level-1 units.

Since all outcomes were continuous, we used a unit link function and measurement model

$$y_i = \mathbf{d}'_{s,i} \boldsymbol{\beta}_s + d_{h,i} \{ \mathbf{x}'_{h,i} \boldsymbol{\beta}_h + f(a_i) \} + \eta_1^{(2)} \mathbf{z}'_i \boldsymbol{\lambda}_1 + d_{h,i} \eta_2^{(2)} + \epsilon_i, \quad (36)$$

where $\boldsymbol{\beta}_s$ contains the intercepts for the items measuring socioeconomic status and $\mathbf{d}_{s,i}$ is vector whose k th element is an indicator for the event that the i th level-1 unit measures the k th socioeconomic status item. Variable $d_{h,i} \in \{0, 1\}$ indicates the event that the i th level-1 unit is a measurement of hippocampal volume, $\mathbf{x}_{h,i}$ is a vector of linear regression terms for scanner, sex, and intracranial volume, and $\boldsymbol{\beta}_h$ are corresponding regression coefficients. The age of the participant to which the i th level-1 unit belongs is denoted a_i , and $f(\cdot)$ is a smooth function composed as a linear combination of fifteen cubic regression splines according to (5). Latent socioeconomic status is represented by $\eta_1^{(2)}$, and $\boldsymbol{\lambda}_1 = (\lambda_1, \dots, \lambda_8)'$ is a vector of factor loadings. Factor loadings for paternal, maternal, and the participant's own education level were represented by $\lambda_1, \dots, \lambda_3$, and the corresponding factor loadings for paternal, maternal, and the participant's own income were represented by $\lambda_4, \dots, \lambda_6$. Accordingly, when the i th level-1 unit is a measurement of income or education, \mathbf{z}_i is an indicator vector which ensures that the correct factor loading among $\lambda_1, \dots, \lambda_6$ is multiplied by $\eta_1^{(2)}$. Finally, λ_7 represented the effect of latent socioeconomic status on hippocampal volume, and λ_8 the interaction effect of age and socioeconomic status on hippocampal volume. Hence, when the i th level-1 unit is a measurement of hippocampal volume, $\mathbf{z}'_i = (0, \dots, 0, 1, a_i)$. Since the data contained repeated scans, a random intercept for hippocampal volume $\eta_2^{(2)}$ was also included. A heteroscedastic model for the residuals was assumed, $\epsilon_i \sim N(0, \sigma_{g(i)}^2)$, where $g(i) = 1$ if the i th level-1 unit is a measurement of income, $g(i) = 2$ if it is a measurement of education level, and $g(i) = 3$ if it is a measurement of hippocampal volume. The structural model was simply $\boldsymbol{\eta}^{(2)} = \boldsymbol{\zeta}^{(2)} \sim N(\mathbf{0}, \boldsymbol{\Psi}^{(2)})$ where $\boldsymbol{\Psi}^{(2)} = \text{diag}(\psi_1^{(2)}, \psi_2^{(2)})$. Assuming zero correlation between level-2 disturbances was required for identifiability, since $\eta_2^{(2)}$ depends on $\eta_1^{(2)}$ through λ_7 and λ_8 .

The model was estimated with the profile likelihood method of Section 2.4, using the `gamm()` function from 'mgcv' (Wood, 2017) in step (26), as it allows heteroscedastic residuals. Since we used a unit link function and normally distributed residuals, it returns exact maximum likelihood estimates. Income and education variables were log-transformed to obtain response values closer to a normal distribution. When fitting the models, all quantitative variables were transformed to have zero mean and unit standard deviations. For identifiability, λ_1 was fixed to unity on the transformed scale used in model fitting. The model described above has seven free factor loadings, $\lambda_2, \dots, \lambda_8$, and we compared it to constrained versions using the marginal

Akaike information criterion (AIC). Since the models differed only in terms of the number of factor loadings, the degrees of freedom were appropriately defined as the number of fixed effect (Vaida and Blanchard, 2005). Based on the results shown in Table 2 we chose model (f), with equal loadings for the education items, equal loadings for the income items, and no interaction effect between age and socioeconomic status on hippocampal volume.

Table 3 shows the estimated parametric effects of main interest. Item intercepts β_s can be found in Supplementary Table S1. Standard errors are not reported for variance components, as their likelihood is typically not regular. We note that naive standard errors were very close to the asymptotic standard errors for all parameters, and as expected, higher total intracranial volume and being male were associated with higher hippocampal volume. From the estimated standard deviation of the random intercept for hippocampal volume and the residual standard deviation for hippocampal volume, we find an intraclass correlation (ICC) of $= 600^2 / (600^2 + 133^2) = 0.95$. An ICC this high implies that the variation between individuals is much larger than the variation between different timepoints of the same individual, as is also clear from the raw data plot in Figure 6 (left). The estimated factor loading for income was positive, with 95% confidence interval $[0.16, 0.37]$, indicating that both education and income are positively related to the latent construct $\eta_1^{(2)}$. It also follows that the difference between mean socioeconomic status and a socioeconomic status one standard deviation above the mean is associated with a difference in education level of $\exp(\hat{\beta}_{s3} + \hat{\lambda}_3 \sqrt{\hat{\psi}_1^{(2)}}) - \exp(\hat{\beta}_{s3}) = 2$ years and with difference in annual income of $\exp(\hat{\beta}_{s6} + \hat{\lambda}_6 \sqrt{\hat{\psi}_1^{(2)}}) - \exp(\hat{\beta}_{s6}) = 95 \times 10^3$ NOK, where we have taken $\hat{\beta}_{s3} = 2.81$ and $\hat{\beta}_{s6} = 13.1$ from Supplementary Table S1. Note that this effect is not additive on the natural scale, since education and income levels were log-transformed.

Figure 6 (right) shows the estimated hippocampal trajectories at three levels of socioeconomic status. From Table 3, the estimated main effect of socioeconomic status on hippocampal volume, $\hat{\lambda}_7$ had 95% confidence interval containing zero, $[-5.3, 121.7]$ mm³, and is hence not significant at a 5% level. From the point estimate, we see that a one standard deviation increase in socioeconomic status is associated with an increase in hippocampal volume of $\hat{\lambda}_7 \sqrt{\hat{\psi}_1^{(2)}} = 39$ mm³. For comparison, the rate of increase seen during childhood in Figure 6 (left) is around 50 mm³/year, the rate of decline during adulthood around 10-15 mm³/year, increasing to 90-100 mm³/year in old age. Assuming no birth cohort effects and representative sampling, the presence of a constant effect λ_7 and the absence of an interaction effect λ_8 , would imply that socioeconomic status affects early life brain development, rather than the rate of change at any point later in life. However, this analysis is inconclusive with regards to such a conclusion.

3.3.2 Simulation Experiments

Simulation experiments were performed based on the model estimated in the previous section. In particular, we were interested in understanding model selection with AIC as performed in Table 2 and the estimation of hippocampal volume trajectories as in Figure 6 (right). To this end, we simulated data using estimated model parameters and a data structure closely following the real data, as shown in Supplementary Figures S2 and S3. For simplicity, explanatory variables related to scanner, sex, and intracranial volume were not included in the simulations, but otherwise the model was identical to (36), with parameter values reported in Table 3 and Supplementary Table S1. The simulations were repeated with six discrete values of the interaction parameter λ_8 , ranging from 0 to 0.12. Zero interaction implies that the trajectories for different levels of socioeconomic status are parallel, as in Figure 6 (right), whereas a positive interaction implies that high socioeconomic status is associated with a slower rate of aging in adulthood. This is illustrated in Supplementary Figure S13. For all parameter settings, 500 Monte Carlo samples with 1886 participants were randomly sampled, and models corresponding to (e) and (f) in Table 2 were fitted.

Figure 7 (left) shows the performance of model selection with AIC and model selection with a one-sided hypothesis test at 5% significance level. That is, models (e) and (f) in Table 2 were compared. With true interaction zero, the probability of falsely rejecting the null hypothesis $\lambda_8 = 0$ was around 5%, and the probability of AIC selecting the model containing this interaction term is close to the expected value of 16%. Furthermore, the curves suggest that we would have around 80% power to detect a moderate interaction $\lambda_8 \approx 0.07$. Figure 7 (right) shows the distribution of estimates $\hat{\lambda}_8$ in the larger model (e) over all Monte Carlo samples. It is evident that the estimated interactions are symmetrically distributed around their true values. Also for the other factor loadings in the model, the estimates had low bias and close to nominal coverage of confidence intervals, as shown in Supplementary Figures S11 and S12. An exception was the effect of socioeconomic status on hippocampal volume λ_7 , which was biased and had below nominal coverage in model (f) when the true interaction λ_8 was large. However, in this case model (f) is misspecified, and as suggested by Figure 7 (left), the correct model (e) would be chosen with high probability. Finally, we investigated pointwise confidence intervals for lifespan trajectories at latent socioeconomic status equal to the mean or one or two standard deviations above or below mean, corresponding to the curves in Figure 6 (right). As shown in Figure 8, the pointwise confidence intervals had close to nominal coverage, whereas the simultaneous confidence intervals in general were conservative, with coverage above 95%.

4 Discussion

We have presented the GALAMM framework for multilevel latent variable modeling, which combines structural equation and item response models’ ability to accurately model a measurement process with generalized additive models’ ability to flexibly estimate smooth functional relationships. As shown in Section 2.2, any GALAMM can be transformed to a GLLAMM (Rabe-Hesketh et al., 2004a), with smoothing parameters represented as variance components and estimated by maximum likelihood. We proposed a profile likelihood algorithm for model fitting, extending the ideas of Jeon and Rabe-Hesketh (2012). The simulation experiments reported in Sections 3.1.2 and 3.3.2 suggest that the algorithm has low bias even with moderate sample sizes, and that confidence intervals derived from the asymptotic standard error formulas in Section 2.5 have close to nominal coverage.

In Section 3 we showed three example applications, illustrating how the models can be used to solve problems in cognitive neuroscience. A number of extensions of the presented models are possible within the framework, and might be relevant depending on the available data and the research questions to be investigated. In Section 3.1.1, the magnitude of retest effects can be expected to depend both on time since last test and on the number of tests taken, and this could be incorporated by including further parametric terms in the measurement model. See Ghisletta and de Ribaupierre (2005) for an example. We also assumed measurement invariance across age (Horn and Mcardle, 1992). This could be relaxed with age-dependent factor loadings, by extending the term $\mathbf{z}_i'\boldsymbol{\lambda}$ in the measurement model (31) to have elements $\lambda_i + a\lambda_a$, where a is the participant’s age and λ_a is an age effect common to all items. This would be a non-uniform differential item functioning model (Jeon and Rabe-Hesketh, 2012; Swaminathan and Rogers, 1990). In the factor-by-curve model in Section 3.2.1, random slopes of age could be included at level 3, allowing estimation of how individual change is correlated across cognitive domains as well as level-slope correlation within domains. These topics were studied in a recent meta analysis (Tucker-Drob et al., 2019) in which all the contributing studies had analyzed samples of adults using linear models. GALAMM would more easily allow such studies of coupled cognitive change across the lifespan, since the nonlinear effect of age is flexibly handled by smooth terms.

An extension of the latent covariates model in Section 3.3.1 would be to estimate the effect of socioeconomic status on a larger number of brain regions. Smoothing parameters could be shared as in Section 3.2.1, and the impact of socioeconomic status investigated for each brain region. Including a larger number of indicators of socioeconomic status would likely also increase statistical power, and with the mixed response approach discussed in the next paragraph this could also include ordinal and categorical responses, e.g., occupation. We used marginal AIC for selecting fixed effects. For smooth terms, conditional AIC

with correction for smoothing parameter uncertainty would be appropriate. The method of Wood et al. (2016) for computing the conditional AIC requires the covariance matrix of the log smoothing parameter, which can be obtained from the covariance of the corresponding variance components in (28), using a proper transformation of variables.

A final comment to the models in Section 3 is that while scientific interest typically concerns longitudinal effects, in the presence of birth cohort effects the estimated trajectories in Figure 2 (right), Figure 5 (left), and Figure 6 (right) represent a combination of longitudinal and cross-sectional information (Fitzmaurice et al., 2011, Ch. 9.5). Sørensen et al. (2021) investigated this issue for GAMMs, and found that including birth year as an additional term typically is preferable to the more common approach in linear models of splitting age into a baseline term and a time-since-baseline term.

The GALAMM framework naturally accommodates models with responses of different type, e.g., combinations of continuous, ordinal, and binomial responses, by letting the link function in the response distribution (3) vary with level-1 unit i . A practical limitation is the lack of available software for maximum likelihood estimation of GLMMs with mixed responses. The large number of random effects in the typical applications of interest, combined with the fact that the mixed model formulations have three or four levels, makes it challenging to write efficient code to fit the models directly. With fully Bayesian methods, models with mixed response types is possible, e.g., using 'brms' (Bürkner, 2017). However, there are substantial differences between Bayesian and frequentist interpretations, and in some applications, e.g. frequentist control of long-term error rates may be desired. An alternative approach to handling multiple response types is offered by latent response models (Muthén, 1984), in which, e.g., ordinal or binomial responses are assumed to be thresholded realizations of a continuous latent response. A model accommodating both continuous and ordinal responses with a latent response formulation was presented by Fahrmeir and Raach (2007), who used Bayesian P-splines (Lang and Brezger, 2004) to model the effect of age and location on a set of latent variables.

An alternative to the proposed profile likelihood algorithm is to directly maximize the log-likelihood of the nonlinear mixed model in the reduced form (24). The main computational hurdle is to evaluate the likelihood function, which requires integrating over all latent variables. As GALAMMs with smooth terms always have one more hierarchical level than a corresponding GLLAMM, these integrals become increasingly challenging. Rabe-Hesketh et al. (2005) suggested an adaptive Gauss-Hermite quadrature algorithm for numerical integration, which can be combined with quasi-Newton methods like L-BFGS-B. Unfortunately, the algorithm is not currently available in R, but we will address this in future work.

Data and Code Availability Statement

Complete source code for reproducing the simulation results can be found at <https://github.com/LCBC-UiO/galamm-scripts>. Due to privacy concerns, the data used in the examples cannot be publicly shared, however, the repository contains simulated datasets which can be used to rerun all applications and reproduce plots and tables with comparable results. An R package implementing the methods is under development, and available from <https://github.com/LCBC-UiO/galamm>.

Acknowledgement

The data collection was supported by the European Research Council under grant agreements 283634, 725025 (to A.M.F.) and 313440 (to K.B.W.), the Norwegian Research Council (to A.M.F., K.B.W.), The National Association for Public Health’s dementia research program, Norway (to A.M.F) and center support from the University of Oslo.

References

- Akaike, H. (1974). A new look at the statistical model identification. *IEEE Transactions on Automatic Control*, 19(6):716–723.
- Alfaro-Almagro, F., McCarthy, P., Afyouni, S., Andersson, J. L. R., Bastiani, M., Miller, K. L., Nichols, T. E., and Smith, S. M. (2021). Confound modelling in UK Biobank brain imaging. *NeuroImage*, 224:117002.
- Arminger, G. and Muthén, B. O. (1998). A Bayesian approach to nonlinear latent variable models using the Gibbs sampler and the Metropolis-Hastings algorithm. *Psychometrika*, 63(3):271–300.
- Arnold, J. B. (2021). ggthemes: Extra themes, scales and geoms for ‘ggplot2’. R package version 4.2.4.
- Baltes, P. B. (1968). Longitudinal and Cross-Sectional Sequences in the Study of Age and Generation Effects. *Human Development*, 11(3):145–171.
- Bates, D., Mächler, M., Bolker, B., and Walker, S. (2015). Fitting Linear Mixed-Effects Models Using lme4. *Journal of Statistical Software*, 67(1):1–48.
- Bauer, D. J. (2005). A Semiparametric Approach to Modeling Nonlinear Relations Among Latent Variables. *Structural Equation Modeling: A Multidisciplinary Journal*, 12(4):513–535.

- Bengtsson, H. (2021). A unifying framework for parallel and distributed processing in R using futures. *R Journal*.
- Bernal-Rusiel, J. L., Reuter, M., Greve, D. N., Fischl, B., and Sabuncu, M. R. (2013). Spatiotemporal linear mixed effects modeling for the mass-univariate analysis of longitudinal neuroimage data. *NeuroImage*, 81:358–370.
- Blackburn, H. L. and Benton, A. L. (1959). Revised administration and scoring of the Digit Span Test. *Journal of Consulting Psychology*, 21(2):139.
- Bollen, K. A. and Curran, P. J. (2006). *Latent Curve Models: A Structural Equation Perspective*. Wiley Series in Probability and Statistics. John Wiley & Sons, Hoboken, N.J.
- Borchers, D. L., Buckland, S. T., Priede, I. G., and Ahmadi, S. (1997). Improving the precision of the daily egg production method using generalized additive models. *Canadian Journal of Fisheries and Aquatic Sciences*, 54(12):2727–2742.
- Bowman, F. D. (2007). Spatiotemporal Models for Region of Interest Analyses of Functional Neuroimaging Data. *Journal of the American Statistical Association*, 102(478):442–453.
- Breslow, N. E. and Clayton, D. G. (1993). Approximate Inference in Generalized Linear Mixed Models. *Journal of the American Statistical Association*, 88(421):9–25.
- Brezger, A. and Lang, S. (2006). Generalized structured additive regression based on Bayesian P-splines. *Computational Statistics & Data Analysis*, 50(4):967–991.
- Brumback, B. A., Brumback, L. C., and Lindstrom, M. J. (2009). Penalized spline models for longitudinal data. In Fitzmaurice, G., Davidian, M., Verbeke, G., and Molenberghs, G., editors, *Longitudinal Data Analysis*, pages 291–316. Chapman and Hall, London, U.K.
- Bürkner, P.-C. (2017). brms: An R Package for Bayesian Multilevel Models Using Stan. *Journal of Statistical Software*, 80(1):1–28.
- Bürkner, P.-C. (2018). Advanced Bayesian Multilevel Modeling with the R Package brms. *The R Journal*, 10(1):395–411.
- Busemeyer, J. R. and Jones, L. E. (1983). Analysis of multiplicative combination rules when the causal variables are measured with error. *Psychological Bulletin*, 93(3):549–562.
- Byrd, R. H., Lu, P., Nocedal, J., and Zhu, C. (1995). A Limited Memory Algorithm for Bound Constrained Optimization. *SIAM Journal on Scientific Computing*, 16(5):1190–1208.

- Carroll, R. J., Ruppert, D., Stefanski, L. A., and Crainiceanu, C. M. (2006). *Measurement Error in Nonlinear Models: A Modern Perspective*. Monographs on Statistics and Applied Probability. John Wiley & Sons, Boca Raton, Florida, second edition.
- Catalano, P. J. and Ryan, L. M. (1992). Bivariate Latent Variable Models for Clustered Discrete and Continuous Outcomes. *Journal of the American Statistical Association*, 87(419):651–658.
- Comets, E., Lavenu, A., and Lavielle, M. (2017). Parameter Estimation in Nonlinear Mixed Effect Models Using saemix, an R Implementation of the SAEM Algorithm. *Journal of Statistical Software*, 80(1):1–41.
- Coull, B. A., Ruppert, D., and Wand, M. P. (2001). Simple Incorporation of Interactions into Additive Models. *Biometrics*, 57(2):539–545.
- Curran, P. J. (2003). Have Multilevel Models Been Structural Equation Models All Along? *Multivariate Behavioral Research*, 38(4):529–569.
- Curran, P. J. and Bauer, D. J. (2011). The disaggregation of within-person and between-person effects in longitudinal models of change. *Annual Review of Psychology*, 62(1):583–619.
- Dale, A. M., Fischl, B., and Sereno, M. I. (1999). Cortical Surface-Based Analysis: I. Segmentation and Surface Reconstruction. *NeuroImage*, 9(2):179–194.
- Davidian, M. (2009). Non-linear Mixed Effects Models. In Fitzmaurice, G., Davidian, M., Verbeke, G., and Molenberghs, G., editors, *Longitudinal Data Analysis*, pages 107–142. Chapman and Hall, London, U.K.
- Delis, D. C., Kramer, J. H., Kaplan, E., and Ober, B. A. (1987). *CVLT, California Verbal Learning Test*. Psychological Corporation, San Antonio, TX.
- Delis, D. C., Kramer, J. H., Kaplan, E., and Ober, B. A. (2000). *CVLT, California Verbal Learning Test: Second Edition*. Psychological Corporation, San Antonio, TX.
- Delyon, B., Lavielle, M., and Moulines, E. (1999). Convergence of a Stochastic Approximation Version of the EM Algorithm. *The Annals of Statistics*, 27(1):94–128.
- Demidenko, E. (2013). *Mixed Models: Theory and Applications with R*. Wiley Series in Probability and Statistics. John Wiley & Sons, Hoboken, N.J., second edition.
- Dempster, A. P., Laird, N. M., and Rubin, D. B. (1977). Maximum Likelihood from Incomplete Data Via the EM Algorithm. *Journal of the Royal Statistical Society: Series B (Methodological)*, 39(1):1–22.

- Dominici, F., McDermott, A., Zeger, S. L., and Samet, J. M. (2002). On the Use of Generalized Additive Models in Time-Series Studies of Air Pollution and Health. *American Journal of Epidemiology*, 156(3):193–203.
- Driver, C. C. and Voelkle, M. C. (2018). Hierarchical Bayesian continuous time dynamic modeling. *Psychological Methods*, 23(4):774–799.
- Dubois, B., Hampel, H., Feldman, H. H., Scheltens, P., Aisen, P., Andrieu, S., Bakardjian, H., Benali, H., Bertram, L., Blennow, K., Broich, K., Cavedo, E., Crutch, S., Dartigues, J.-F., Duyckaerts, C., Epelbaum, S., Frisoni, G. B., Gauthier, S., Genthon, R., Gouw, A. A., Habert, M.-O., Holtzman, D. M., Kivipelto, M., Lista, S., Molinuevo, J.-L., O’Bryant, S. E., Rabinovici, G. D., Rowe, C., Salloway, S., Schneider, L. S., Sperling, R., Teichmann, M., Carrillo, M. C., Cummings, J., Jack Jr, C. R., and Proceedings of the Meeting of the International Working Group (IWG) and the American Alzheimer’s Association on “The Preclinical State of AD”; July 23, USA, . W. D. (2016). Preclinical Alzheimer’s disease: Definition, natural history, and diagnostic criteria. *Alzheimer’s & Dementia*, 12(3):292–323.
- Duff, K., Westervelt, H. J., McCaffrey, R. J., and Haase, R. F. (2001). Practice effects, test–retest stability, and dual baseline assessments with the California Verbal Learning Test in an HIV sample. *Archives of Clinical Neuropsychology*, 16(5):461–476.
- Edwards, J. R. and Bagozzi, R. P. (2000). On the nature and direction of relationships between constructs and measures. *Psychological Methods*, 5(2):155–174.
- Estrada, E. and Ferrer, E. (2019). Studying developmental processes in accelerated cohort-sequential designs with discrete- and continuous-time latent change score models. *Psychological Methods*, 24(6):708–734.
- Fahrmeir, L. and Raach, A. (2007). A Bayesian Semiparametric Latent Variable Model for Mixed Responses. *Psychometrika*, 72(3):327.
- Fieuws, S. and Verbeke, G. (2006). Pairwise Fitting of Mixed Models for the Joint Modeling of Multivariate Longitudinal Profiles. *Biometrics*, 62(2):424–431.
- Fieuws, S. and Verbeke, G. (2009). Joint models for high-dimensional longitudinal data. In Fitzmaurice, G., Davidian, M., Verbeke, G., and Molenberghs, G., editors, *Longitudinal Data Analysis*, pages 367–391. Chapman and Hall, London, U.K.
- Fischl, B., Salat, D. H., Busa, E., Albert, M., Dieterich, M., Haselgrove, C., van der Kouwe, A., Killiany, R., Kennedy, D., Klaveness, S., Montillo, A., Makris, N., Rosen, B., and Dale, A. M. (2002). Whole

- Brain Segmentation: Automated Labeling of Neuroanatomical Structures in the Human Brain. *Neuron*, 33(3):341–355.
- Fitzmaurice, G. M., Laird, N. M., and Ware, J. H. (2011). *Applied Longitudinal Analysis*. Wiley Series in Probability and Statistics. John Wiley & Sons, Hoboken, N.J., 2nd edition edition.
- Fjell, A. M., Idland, A.-V., Sala-Llloch, R., Watne, L. O., Borza, T., Brækhus, A., Lona, T., Zetterberg, H., Blennow, K., Wyller, T. B., and Walhovd, K. B. (2018). Neuroinflammation and Tau Interact with Amyloid in Predicting Sleep Problems in Aging Independently of Atrophy. *Cerebral Cortex*, 28(8):2775–2785.
- Fjell, A. M., Walhovd, K. B., Westlye, L. T., Østby, Y., Tamnes, C. K., Jernigan, T. L., Gamst, A., and Dale, A. M. (2010). When does brain aging accelerate? Dangers of quadratic fits in cross-sectional studies. *NeuroImage*, 50(4):1376–1383.
- Ganguli, B., Staudenmayer, J., and Wand, M. P. (2005). Additive Models with Predictors Subject to Measurement Error. *Australian & New Zealand Journal of Statistics*, 47(2):193–202.
- Genz, A., Bretz, F., Miwa, T., Mi, X., Leisch, F., Scheipl, F., and Hothorn, T. (2020). *mvtnorm: Multivariate Normal and t Distributions*. R package version 1.1-1.
- Ghisletta, P. and de Ribaupierre, A. (2005). A dynamic investigation of cognitive dedifferentiation with control for retest: Evidence from the Swiss Interdisciplinary Longitudinal Study on the Oldest Old. *Psychology and Aging*, 20(4):671–682.
- Gilbert, P. and Varadhan, R. (2019). *numDeriv: Accurate Numerical Derivatives*. R package version 2016.8-1.1.
- Gong, G. and Samaniego, F. J. (1981). Pseudo Maximum Likelihood Estimation: Theory and Applications. *The Annals of Statistics*, 9(4):861–869.
- Greven, S. and Kneib, T. (2010). On the behaviour of marginal and conditional AIC in linear mixed models. *Biometrika*, 97(4):773–789.
- Gueorguieva, R. (2001). A multivariate generalized linear mixed model for joint modelling of clustered outcomes in the exponential family. *Statistical Modelling*, 1(3):177–193.
- Hadfield, J. D. (2010). MCMC Methods for Multi-Response Generalized Linear Mixed Models: The MCMCglmm R Package. *Journal of Statistical Software*, 33(1):1–22.

- Hall, P. and Opsomer, J. D. (2005). Theory for penalised spline regression. *Biometrika*, 92(1):105–118.
- Hanson, J. L., Chandra, A., Wolfe, B. L., and Pollak, S. D. (2011). Association between Income and the Hippocampus. *PLOS ONE*, 6(5):e18712.
- Hastie, T. and Tibshirani, R. (1986). Generalized Additive Models. *Statistical Science*, 1(3):297–310.
- Hastie, T. and Tibshirani, R. (1993). Varying-Coefficient Models. *Journal of the Royal Statistical Society: Series B (Methodological)*, 55(4):757–779.
- Hintze, J. L. and Nelson, R. D. (1998). Violin Plots: A Box Plot-Density Trace Synergism. *The American Statistician*, 52(2):181–184.
- Horn, J. L. and Mcardle, J. J. (1992). A practical and theoretical guide to measurement invariance in aging research. *Experimental Aging Research*, 18(3):117–144.
- Hyatt, C. S., Owens, M. M., Crowe, M. L., Carter, N. T., Lynam, D. R., and Miller, J. D. (2020). The quandary of covarying: A brief review and empirical examination of covariate use in structural neuroimaging studies on psychological variables. *NeuroImage*, 205:116225.
- Ivanova, A., Molenberghs, G., and Verbeke, G. (2016). Mixed models approaches for joint modeling of different types of responses. *Journal of Biopharmaceutical Statistics*, 26(4):601–618.
- Jeon, M. and Rabe-Hesketh, S. (2012). Profile-Likelihood Approach for Estimating Generalized Linear Mixed Models With Factor Structures. *Journal of Educational and Behavioral Statistics*, 37(4):518–542.
- Jöreskog, K. G. (1969). A general approach to confirmatory maximum likelihood factor analysis. *Psychometrika*, 34(2):183–202.
- Jöreskog, K. G. (1970). A General Method for Estimating a Linear Structural Equation System. *ETS Research Bulletin Series*, 1970(2):i–41.
- Kelava, A. and Brandt, H. (2014). A general non-linear multilevel structural equation mixture model. *Frontiers in Psychology*, 5.
- Kelava, A., Nagengast, B., and Brandt, H. (2014). A Nonlinear Structural Equation Mixture Modeling Approach for Nonnormally Distributed Latent Predictor Variables. *Structural Equation Modeling: A Multidisciplinary Journal*, 21(3):468–481.
- Kenny, D. A. and Judd, C. M. (1984). Estimating the nonlinear and interactive effects of latent variables. *Psychological Bulletin*, 96(1):201–210.

- Kievit, R. A., Brandmaier, A. M., Ziegler, G., van Harmelen, A.-L., de Mooij, S. M. M., Moutoussis, M., Goodyer, I. M., Bullmore, E., Jones, P. B., Fonagy, P., Lindenberger, U., and Dolan, R. J. (2018). Developmental cognitive neuroscience using latent change score models: A tutorial and applications. *Developmental Cognitive Neuroscience*, 33:99–117.
- Kimeldorf, G. S. and Wahba, G. (1970). A Correspondence Between Bayesian Estimation on Stochastic Processes and Smoothing by Splines. *Annals of Mathematical Statistics*, 41(2):495–502.
- Klein, N., Kneib, T., Klasen, S., and Lang, S. (2015). Bayesian structured additive distributional regression for multivariate responses. *Journal of the Royal Statistical Society. Series C (Applied Statistics)*, 64(4):569–591.
- Komsta, L. and Novomestky, F. (2015). *moments: Moments, Cumulants, Skewness, Kurtosis and Related Tests*. R package version 0.14.
- Laird, N. M. and Ware, J. H. (1982). Random-Effects Models for Longitudinal Data. *Biometrics*, 38(4):963–974.
- Lang, S. and Brezger, A. (2004). Bayesian P-Splines. *Journal of Computational and Graphical Statistics*, 13(1):183–212.
- Lee, S.-Y. and Zhu, H.-T. (2000). Statistical analysis of nonlinear structural equation models with continuous and polytomous data. *British Journal of Mathematical and Statistical Psychology*, 53(2):209–232.
- Lin, X. and Zhang, D. (1999). Inference in generalized additive mixed models by using smoothing splines. *Journal of the Royal Statistical Society: Series B (Statistical Methodology)*, 61(2):381–400.
- Lindstrom, M. J. and Bates, D. M. (1990). Nonlinear Mixed Effects Models for Repeated Measures Data. *Biometrics*, 46(3):673–687.
- Livingston, G., Sommerlad, A., Orgeta, V., Costafreda, S. G., Huntley, J., Ames, D., Ballard, C., Banerjee, S., Burns, A., Cohen-Mansfield, J., Cooper, C., Fox, N., Gitlin, L. N., Howard, R., Kales, H. C., Larson, E. B., Ritchie, K., Rockwood, K., Sampson, E. L., Samus, Q., Schneider, L. S., Selbæk, G., Teri, L., and Mukadam, N. (2017). Dementia prevention, intervention, and care. *The Lancet*, 390(10113):2673–2734.
- Mair, P. (2018). Path Analysis and Structural Equation Models. In Mair, P., editor, *Modern Psychometrics with R, Use R!*, pages 63–93. Springer International Publishing, Cham.
- Marra, G. and Wood, S. N. (2012). Coverage Properties of Confidence Intervals for Generalized Additive Model Components. *Scandinavian Journal of Statistics*, 39(1):53–74.

- Mayo, D. G. (2018). *Statistical Inference as Severe Testing: How to Get Beyond the Statistics Wars*. Cambridge University Press, Cambridge, UK, 1st edition.
- McArdle, J. J. and Epstein, D. (1987). Latent Growth Curves within Developmental Structural Equation Models. *Child Development*, 58(1):110–133.
- McArdle, J. J., Ferrer-Caja, E., Hamagami, F., and Woodcock, R. W. (2002). Comparative longitudinal structural analyses of the growth and decline of multiple intellectual abilities over the life span. *Developmental Psychology*, 38(1):115–142.
- McCullagh, P. and Nelder, J. A. (1989). *Generalized Linear Models*. Chapman & Hall / CRC, London.
- Mehta, P. D. and Neale, M. C. (2005). People are variables too: Multilevel structural equations modeling. *Psychological Methods*, 10(3):259–284.
- Mehta, P. D. and West, S. G. (2000). Putting the individual back into individual growth curves. *Psychological Methods*, 5(1):23–43.
- Meredith, M. and Kruschke, J. (2020). *HDInterval: Highest (Posterior) Density Intervals*. R package version 0.2.2.
- Meredith, W. and Tisak, J. (1990). Latent curve analysis. *Psychometrika*, 55(1):107–122.
- Meschiari, S. (2021). *latex2exp: Use LaTeX Expressions in Plots*. R package version 0.5.0.
- Mislevy, R. J. (1985). Estimation of Latent Group Effects. *Journal of the American Statistical Association*, 80(392):993–997.
- Muthén, B. (1983). Latent variable structural equation modeling with categorical data. *Journal of Econometrics*, 22(1):43–65.
- Muthén, B. (1984). A general structural equation model with dichotomous, ordered categorical, and continuous latent variable indicators. *Psychometrika*, 49(1):115–132.
- Muthén, B. O. (2002). Beyond SEM: General Latent Variable Modeling. *Behaviormetrika*, 29(1):81–117.
- Nash, J. C. (2014). On Best Practice Optimization Methods in R. *Journal of Statistical Software*, 60(1):1–14.
- Nash, J. C. and Varadhan, R. (2011). Unifying Optimization Algorithms to Aid Software System Users: optimx for R. *Journal of Statistical Software*, 43(1):1–14.

- Nelder, J. A. and Mead, R. (1965). A Simplex Method for Function Minimization. *The Computer Journal*, 7(4):308–313.
- Newcombe, R. G. (1998). Two-sided confidence intervals for the single proportion: Comparison of seven methods. *Statistics in Medicine*, 17(8):857–872.
- Nilsson, L.-G., Sternäng, O., Rönnlund, M., and Nyberg, L. (2009). Challenging the notion of an early-onset of cognitive decline. *Neurobiology of Aging*, 30(4):521–524.
- Noble, K. G., Houston, S. M., Kan, E., and Sowell, E. R. (2012). Neural correlates of socioeconomic status in the developing human brain. *Developmental Science*, 15(4):516–527.
- Novick, M. R. (1966). The axioms and principal results of classical test theory. *Journal of Mathematical Psychology*, 3(1):1–18.
- Nyberg, L., Lövdén, M., Riklund, K., Lindenberger, U., and Bäckman, L. (2012). Memory aging and brain maintenance. *Trends in Cognitive Sciences*, 16(5):292–305.
- Nyberg, L., Magnussen, F., Lundquist, A., Baaré, W., Bartrés-Faz, D., Bertram, L., Boraxbekk, C. J., Brandmaier, A. M., Drevon, C. A., Ebmeier, K., Ghisletta, P., Henson, R. N., Junqué, C., Kievit, R., Kleemeyer, M., Knights, E., Kühn, S., Lindenberger, U., Penninx, B. W. J. H., Pudas, S., Sørensen, Ø., Vaqué-Alcázar, L., Walhovd, K. B., and Fjell, A. M. (2021). Educational attainment does not influence brain aging. *Proceedings of the National Academy of Sciences*, 118(18).
- Nychka, D. (1988). Bayesian Confidence Intervals for Smoothing Splines. *Journal of the American Statistical Association*, 83(404):1134–1143.
- Ostrosky-Solís, F. and Lozano, A. (2006). Digit Span: Effect of education and culture. *International Journal of Psychology*, 41(5):333–341.
- Oud, J. H. L. and Jansen, R. A. R. G. (2000). Continuous time state space modeling of panel data by means of SEM. *Psychometrika*, 65(2):199–215.
- Paolo, A. M., Tröster, A. I., and Ryan, J. J. (1997). Test–retest stability of the California Verbal Learning Test in older persons. *Neuropsychology*, 11(4):613–616.
- Park, D. C., Lautenschlager, G., Hedden, T., Davidson, N. S., Smith, A. D., and Smith, P. K. (2002). Models of visuospatial and verbal memory across the adult life span. *Psychology and Aging*, 17(2):299–320.
- Parke, W. R. (1986). Pseudo Maximum Likelihood Estimation: The Asymptotic Distribution. *The Annals of Statistics*, 14(1):355–357.

- Pawitan, Y. (2001). *In All Likelihood*. Oxford University Press, New York, NY.
- Pedersen, E. J., Miller, D. L., Simpson, G. L., and Ross, N. (2019). Hierarchical generalized additive models in ecology: An introduction with mgcv. *PeerJ*, 7:e6876.
- Pedersen, T. L. (2020). *patchwork: The Composer of Plots*. R package version 1.1.1.
- Pinheiro, J., Bates, D., DebRoy, S., Sarkar, D., and R Core Team (2020). *nlme: Linear and Nonlinear Mixed Effects Models*. R package version 3.1-150.
- Proust-Lima, C., Amieva, H., and Jacqmin-Gadda, H. (2013). Analysis of multivariate mixed longitudinal data: A flexible latent process approach. *British Journal of Mathematical and Statistical Psychology*, 66(3):470–487.
- Proust-Lima, C., Philipps, V., and Lique, B. (2017). Estimation of Extended Mixed Models Using Latent Classes and Latent Processes: The R Package lcmm. *Journal of Statistical Software*, 78(1):1–56.
- R Core Team (2020). *R: A Language and Environment for Statistical Computing*. R Foundation for Statistical Computing, Vienna, Austria.
- Rabe-Hesketh, S., Skrondal, A., and Pickles, A. (2004a). Generalized multilevel structural equation modeling. *Psychometrika*, 69(2):167–190.
- Rabe-Hesketh, S., Skrondal, A., and Pickles, A. (2004b). GLLMM Manual. *U.C. Berkeley Division of Biostatistics Working Paper Series*.
- Rabe-Hesketh, S., Skrondal, A., and Pickles, A. (2005). Maximum likelihood estimation of limited and discrete dependent variable models with nested random effects. *Journal of Econometrics*, 128(2):301–323.
- Raz, N. and Lindenberger, U. (2011). Only time will tell: Cross-sectional studies offer no solution to the age–brain–cognition triangle: Comment on Salthouse (2011). *Psychological Bulletin*, 137(5):790–795.
- Reuter, M., Schmansky, N. J., Rosas, H. D., and Fischl, B. (2012). Within-subject template estimation for unbiased longitudinal image analysis. *NeuroImage*, 61(4):1402–1418.
- Rockwood, N. J. (2020). Maximum Likelihood Estimation of Multilevel Structural Equation Models with Random Slopes for Latent Covariates. *Psychometrika*, 85(2):275–300.
- Rockwood, N. J. and Jeon, M. (2019). Estimating Complex Measurement and Growth Models Using the R Package PLmixed. *Multivariate Behavioral Research*, 54(2):288–306.

- Rönnlund, M., Nyberg, L., Bäckman, L., and Nilsson, L.-G. (2005). Stability, growth, and decline in adult life span development of declarative memory: Cross-sectional and longitudinal data from a population-based study. *Psychology and Aging*, 20(1):3–18.
- Ruppert, D. and Carroll, R. J. (2000). Theory & Methods: Spatially-adaptive Penalties for Spline Fitting. *Australian & New Zealand Journal of Statistics*, 42(2):205–223.
- Ruppert, D., Wand, M. P., and Carroll, R. J. (2003). *Semiparametric Regression*. Cambridge University Press, Cambridge, U.K.
- Saeften, B., Kneib, T., van Waveren, C.-S., and Greven, S. (2014). A unifying approach to the estimation of the conditional Akaike information in generalized linear mixed models. *Electronic Journal of Statistics*, 8(1):201–225.
- Salthouse, T. A. (2009). When does age-related cognitive decline begin? *Neurobiology of Aging*, 30(4):507–514.
- Salthouse, T. A. (2011). Neuroanatomical substrates of age-related cognitive decline. *Psychological Bulletin*, 137(5):753–784.
- Sammel, M. D., Ryan, L. M., and Legler, J. M. (1997). Latent Variable Models for Mixed Discrete and Continuous Outcomes. *Journal of the Royal Statistical Society: Series B (Statistical Methodology)*, 59(3):667–678.
- Schaie, K. W. (2009). “When does age-related cognitive decline begin?” Salthouse again reifies the “cross-sectional fallacy”. *Neurobiology of Aging*, 30(4):528–529.
- Schall, R. (1991). Estimation in Generalized Linear Models with Random Effects. *Biometrika*, 78(4):719–727.
- Scharfen, J., Peters, J. M., and Holling, H. (2018). Retest effects in cognitive ability tests: A meta-analysis. *Intelligence*, 67:44–66.
- Sheppard, L., Slaughter, J. C., Schildcrout, J., Liu, L.-J. S., and Lumley, T. (2005). Exposure and measurement contributions to estimates of acute air pollution effects. *Journal of Exposure Science & Environmental Epidemiology*, 15(4):366–376.
- Silverman, B. W. (1985). Some Aspects of the Spline Smoothing Approach to Non-Parametric Regression Curve Fitting. *Journal of the Royal Statistical Society: Series B (Methodological)*, 47(1):1–21.
- Skrondal, A. and Rabe-Hesketh, S. (2004). *Generalized Latent Variable Modeling*. Interdisciplinary Statistics Series. Chapman and Hall/CRC, Boca Raton, Florida.

- Skrondal, A. and Rabe-Hesketh, S. (2007). Latent Variable Modelling: A Survey. *Scandinavian Journal of Statistics*, 34(4):712–745.
- Snijders, T. A. B. and Bosker, R. J. (2012). *Multilevel Analysis*. SAGE Publications Ltd, second edition.
- Song, X., Lu, Z., and Feng, X. (2014). Latent variable models with nonparametric interaction effects of latent variables. *Statistics in Medicine*, 33(10):1723–1737.
- Song, X.-Y. and Lu, Z.-H. (2010). Semiparametric Latent Variable Models With Bayesian P-Splines. *Journal of Computational and Graphical Statistics*, 19(3):590–608.
- Song, X.-Y., Lu, Z.-H., Cai, J.-H., and Ip, E. H.-S. (2013). A Bayesian Modeling Approach for Generalized Semiparametric Structural Equation Models. *Psychometrika*, 78(4):624–647.
- Sørensen, Ø., Walhovd, K. B., and Fjell, A. M. (2021). A recipe for accurate estimation of lifespan brain trajectories, distinguishing longitudinal and cohort effects. *NeuroImage*, 226:117596.
- Spearman, C. (1904). "General Intelligence," Objectively Determined and Measured. *The American Journal of Psychology*, 15(2):201–292.
- Speed, T. (1991). [That BLUP is a Good Thing: The Estimation of Random Effects]: Comment. *Statistical Science*, 6(1):42–44.
- Staff, R. T., Murray, A. D., Ahearn, T. S., Mustafa, N., Fox, H. C., and Whalley, L. J. (2012). Childhood socioeconomic status and adult brain size: Childhood socioeconomic status influences adult hippocampal size. *Annals of Neurology*, 71(5):653–660.
- StataCorp (2019). Stata Statistical Software: Release 16. StataCorp LLC.
- Stegmann, G., Jacobucci, R., Harring, J. R., and Grimm, K. J. (2018). Nonlinear Mixed-Effects Modeling Programs in R. *Structural Equation Modeling: A Multidisciplinary Journal*, 25(1):160–165.
- Swaminathan, H. and Rogers, H. J. (1990). Detecting Differential Item Functioning Using Logistic Regression Procedures. *Journal of Educational Measurement*, 27(4):361–370.
- Swamy, P. A. V. B. (1970). Efficient Inference in a Random Coefficient Regression Model. *Econometrica*, 38(2):311–323.
- Swamy, P. A. V. B. (1971). *Statistical Inference in Random Coefficient Regression Models*. Lecture Notes in Economics and Mathematical Systems. Springer-Verlag, Berlin Heidelberg.

- Tiedemann, F. (2020). *gghalves: Compose Half-Half Plots Using Your Favourite Geoms*. R package version 0.1.1.
- Tucker-Drob, E. M. (2019). Cognitive Aging and Dementia: A Life-Span Perspective. *Annual Review of Developmental Psychology*, 1(1):177–196.
- Tucker-Drob, E. M., Brandmaier, A. M., and Lindenberger, U. (2019). Coupled cognitive changes in adulthood: A meta-analysis. *Psychological Bulletin*, 145(3):273–301.
- Vaida, F. and Blanchard, S. (2005). Conditional Akaike information for mixed-effects models. *Biometrika*, 92(2):351–370.
- Vaughan, D. and Dancho, M. (2021). *furrr: Apply Mapping Functions in Parallel Using Futures*. R package version 0.2.2.
- Venables, W. N. and Ripley, B. D. (2002). *Modern Applied Statistics with S*. Springer, New York, fourth edition. ISBN 0-387-95457-0.
- Verbyla, A. P., Cullis, B. R., Kenward, M. G., and Welham, S. J. (1999). The Analysis of Designed Experiments and Longitudinal Data by Using Smoothing Splines. *Journal of the Royal Statistical Society: Series C (Applied Statistics)*, 48(3):269–311.
- Vonesh, E. F. (1996). A note on the use of Laplace’s approximation for nonlinear mixed-effects models. *Biometrika*, 83(2):447–452.
- Walhovd, K. B., Bråthen, A. C. S., Panizzon, M. S., Mowinckel, A. M., Sørensen, Ø., de Lange, A.-M. G., Krogsrud, S. K., Håberg, A., Franz, C. E., Kremen, W. S., and Fjell, A. M. (2020a). Within-session verbal learning slope is predictive of lifespan delayed recall, hippocampal volume, and memory training benefit, and is heritable. *Scientific Reports*, 10(1):21158.
- Walhovd, K. B., Fjell, A. M., Wang, Y., Amlien, I. K., Mowinckel, A. M., Lindenberger, U., Düzel, S., Bartrés-Faz, D., Ebmeier, K. P., Drevon, C. A., Baaré, W., Ghisletta, P., Johansen, L. B., Kievit, R. A., Henson, R. N., Madsen, K. S., Nyberg, L., Harris, J., Solé-Padullés, C., Pudas, S., Sørensen, Ø., West-erhausen, R., Zsoldos, E., Nawijn, L., Lyngstad, T. H., Suri, S., Penninx, B., Røgeberg, O. J., and Brandmaier, A. M. (2020b). Education and income show heterogeneous relationships to lifespan brain and cognitive differences across European and US cohorts. *bioRxiv*, page 2020.10.12.335687.
- Walhovd, K. B., Krogsrud, S. K., Amlien, I. K., Bartsch, H., Bjørnerud, A., Due-Tønnessen, P., Grydeland, H., Hagler, D. J., Håberg, A. K., Kremen, W. S., Ferschmann, L., Nyberg, L., Panizzon, M. S., Rohani,

- D. A., Skranes, J., Storsve, A. B., Sølsnes, A. E., Tamnes, C. K., Thompson, W. K., Reuter, C., Dale, A. M., and Fjell, A. M. (2016). Neurodevelopmental origins of lifespan changes in brain and cognition. *Proceedings of the National Academy of Sciences*, 113(33):9357–9362.
- Wang, T., Graves, B., Rosseel, Y., and Merkle, E. C. (2020). Computation and application of generalized linear mixed model derivatives using lme4. *arXiv:2011.10414 [stat]*.
- Wang, T. and Merkle, E. C. (2018). merDeriv: Derivative Computations for Linear Mixed Effects Models with Application to Robust Standard Errors. *Journal of Statistical Software*, 87(1):1–16.
- Wickham, H. (2016). *ggplot2: Elegant Graphics for Data Analysis*. Springer-Verlag New York.
- Wickham, H. (2019). *stringr: Simple, Consistent Wrappers for Common String Operations*. R package version 1.4.0.
- Wickham, H. (2020). *tidyr: Tidy Messy Data*. R package version 1.1.2.
- Wickham, H., François, R., Henry, L., and Müller, K. (2021). *dplyr: A Grammar of Data Manipulation*. R package version 1.0.4.
- Wickham, H. and Seidel, D. (2020). *scales: Scale Functions for Visualization*. R package version 1.1.1.
- Wieling, M., Tomaschek, F., Arnold, D., Tiede, M., Bröker, F., Thiele, S., Wood, S. N., and Baayen, R. H. (2016). Investigating dialectal differences using articulography. *Journal of Phonetics*, 59:122–143.
- Wilson, E. B. (1927). Probable Inference, the Law of Succession, and Statistical Inference. *Journal of the American Statistical Association*, 22(158):209–212.
- Wood, S. (2017). *Generalized Additive Models: An Introduction with R*. Chapman and Hall/CRC, second edition.
- Wood, S. and Scheipl, F. (2020). *gam4: Generalized Additive Mixed Models Using 'mgcv' and 'lme4'*. R package version 0.2-6.
- Wood, S. N. (2003). Thin Plate Regression Splines. *Journal of the Royal Statistical Society. Series B (Statistical Methodology)*, 65(1):95–114.
- Wood, S. N. (2004). Stable and Efficient Multiple Smoothing Parameter Estimation for Generalized Additive Models. *Journal of the American Statistical Association*, 99(467):673–686.
- Wood, S. N. (2006). Low-Rank Scale-Invariant Tensor Product Smooths for Generalized Additive Mixed Models. *Biometrics*, 62(4):1025–1036.

- Wood, S. N. (2011). Fast stable restricted maximum likelihood and marginal likelihood estimation of semi-parametric generalized linear models. *Journal of the Royal Statistical Society: Series B (Statistical Methodology)*, 73(1):3–36.
- Wood, S. N. (2020). Inference and computation with generalized additive models and their extensions. *TEST*, 29(2):307–339.
- Wood, S. N., Goude, Y., and Shaw, S. (2015). Generalized additive models for large data sets. *Journal of the Royal Statistical Society. Series C (Applied Statistics)*, 64(1):139–155.
- Wood, S. N., Li, Z., Shaddick, G., and Augustin, N. H. (2017). Generalized Additive Models for Gigadata: Modeling the U.K. Black Smoke Network Daily Data. *Journal of the American Statistical Association*, 112(519):1199–1210.
- Wood, S. N., Pya, N., and Säfken, B. (2016). Smoothing Parameter and Model Selection for General Smooth Models. *Journal of the American Statistical Association*, 111(516):1548–1563.
- Wood, S. N., Scheipl, F., and Faraway, J. J. (2013). Straightforward intermediate rank tensor product smoothing in mixed models. *Statistics and Computing*, 23(3):341–360.
- Woods, S. P., Delis, D. C., Scott, J. C., Kramer, J. H., and Holdnack, J. A. (2006). The California Verbal Learning Test – second edition: Test-retest reliability, practice effects, and reliable change indices for the standard and alternate forms. *Archives of Clinical Neuropsychology*, 21(5):413–420.
- Yang, M. and Dunson, D. B. (2010). Bayesian Semiparametric Structural Equation Models with Latent Variables. *Psychometrika*, 75(4):675–693.
- Yee, T. W. and Wild, C. J. (1996). Vector Generalized Additive Models. *Journal of the Royal Statistical Society: Series B (Methodological)*, 58(3):481–493.
- Yu, D. and Yau, K. K. W. (2012). Conditional Akaike information criterion for generalized linear mixed models. *Computational Statistics & Data Analysis*, 56(3):629–644.
- Yu, Q., Daugherty, A. M., Anderson, D. M., Nishimura, M., Brush, D., Hardwick, A., Lacey, W., Raz, S., and Ofen, N. (2018). Socioeconomic status and hippocampal volume in children and young adults. *Developmental Science*, 21(3):e12561.
- Zeger, S. L. and Liang, K.-Y. (1992). An overview of methods for the analysis of longitudinal data. *Statistics in Medicine*, 11(14-15):1825–1839.

List of Figures

1	Number of words recalled in CVLT trials. Observed responses to three of the five items making up the level-1 units in the model of episodic memory considered in Section 3.1. Dots show individual responses, and black lines connect multiple timepoints for the same participant.	42
2	Item characteristic curves and lifespan episodic memory. Left: Item response curves of CVLT trials 1-5. Estimated factor loadings and standard errors are shown by the legend. Shaded regions showing 95% confidence bands are barely visible due to the small standard errors of the factor loadings. Right: Estimate of lifespan episodic memory $h(w)$, with values on y -axis in units of between-subject standard deviation $\sqrt{\hat{\psi}^{(3)}}$. The inner dark shaded regions shows a 95% pointwise confidence interval and the outer light shaded region shows a 95% simultaneous confidence interval.	43
3	Simulation results for parametric terms. All points are averages over 500 Monte Carlo simulations, and error bars show 95% confidence intervals.	44
4	Simulation results for smooth terms. The left plot shows across-the-function coverage of pointwise confidence intervals and coverage of simultaneous confidence intervals. The center plot shows how coverage of pointwise intervals depends on age, and the right plot shows mean-square error, together with its bias-variance decomposition. Error bars and confidence bands represent 95% confidence intervals.	45
5	Lifespan episodic and working memory. Left: Estimated lifespan trajectories of episodic and working memory. Right: Empirical Bayes posterior distribution of the difference in age at maximum of episodic and working memory. Horizontal bar denotes 95% highest posterior density interval.	46
6	Hippocampal volume curves. Left: Total volumes of left and right hippocampus (in mm^3) plotted versus age. Repeated observations of the same individual are connected with gray lines. Right: Estimated hippocampal volume trajectories at mean socioeconomic status (SES) and at two standard deviation above or below mean. Shaded regions show 95% pointwise confidence intervals for SES two standard deviations above or below mean.	47
7	Interaction term in latent covariates model. Left: Probability of selecting a model containing an interaction term as a function of the magnitude of the interaction. 'AIC' denotes Akaike information criterion and ' $p < .05$ ' denotes selection based on testing $\lambda_8 = 0$ versus $\lambda_8 > 0$. Error bars show 95% confidence intervals. Right: Violin-dotplots (Hintze and Nelson, 1998) of estimated interactions for different values of the true interaction. Gray line and black points indicate the true values, and colored points indicate estimates in single Monte Carlo samples. Values are based on 500 Monte Carlo samples for each parameter combination.	48
8	Coverage of smooth terms in latent covariates model. Across-the-function coverage of pointwise confidence intervals (left) and coverage of simultaneous confidence intervals (right) for five levels of latent socioeconomic status $\eta_1^{(2)}$. Intervals were computed with model (e), which contained a non-zero interaction term λ_8 .	49

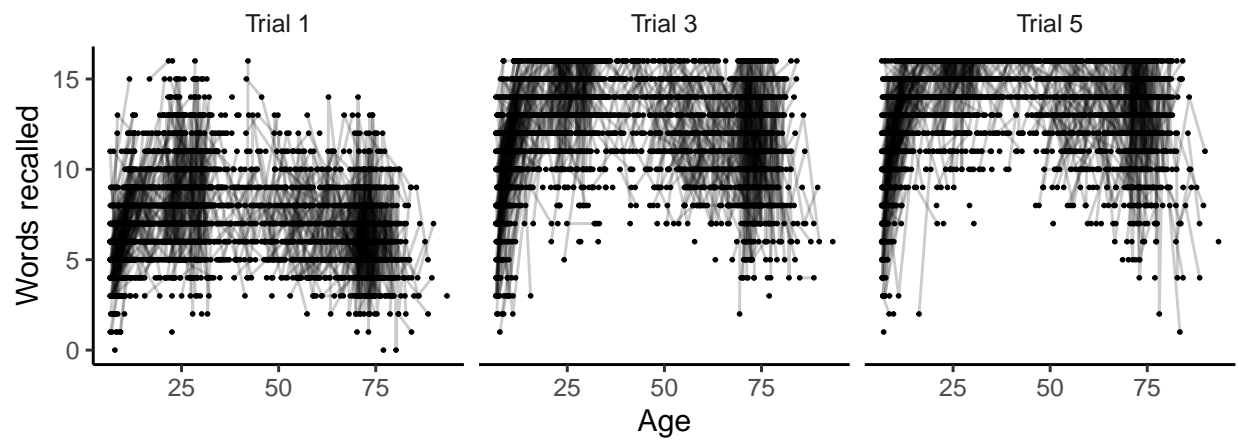


Figure 1: **Number of words recalled in CVLT trials.** Observed responses to three of the five items making up the level-1 units in the model of episodic memory considered in Section 3.1. Dots show individual responses, and black lines connect multiple timepoints for the same participant.

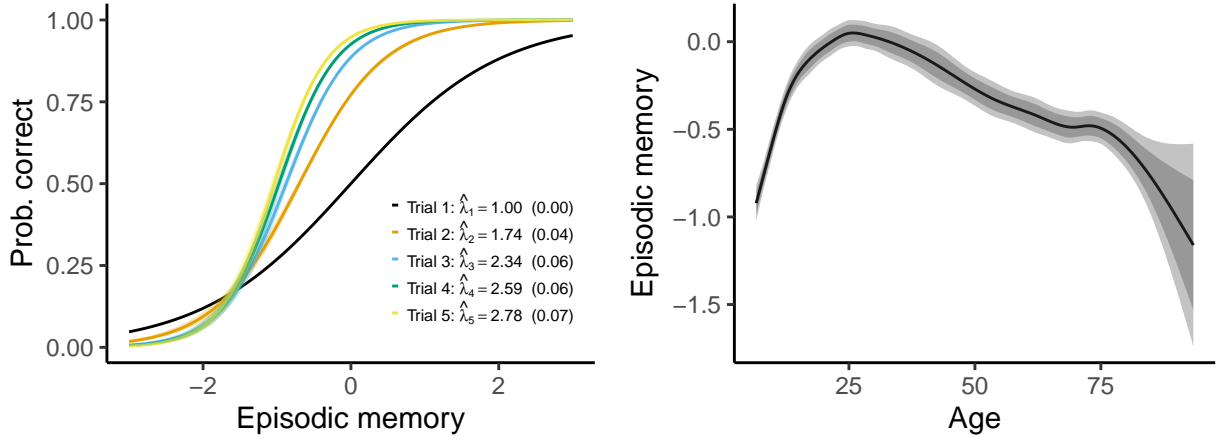
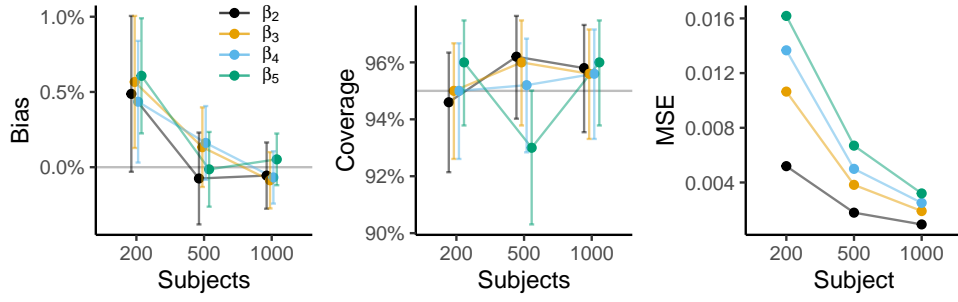
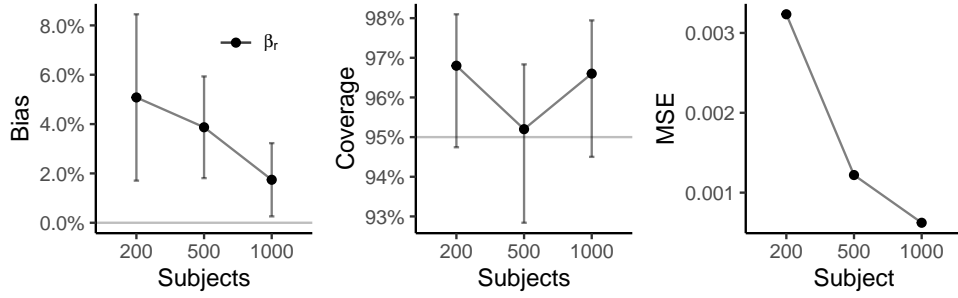


Figure 2: **Item characteristic curves and lifespan episodic memory.** Left: Item response curves of CVLT trials 1-5. Estimated factor loadings and standard errors are shown by the legend. Shaded regions showing 95% confidence bands are barely visible due to the small standard errors of the factor loadings. Right: Estimate of lifespan episodic memory $h(w)$, with values on y -axis in units of between-subject standard deviation $\sqrt{\psi^{(3)}}$. The inner dark shaded regions shows a 95% pointwise confidence interval and the outer light shaded region shows a 95% simultaneous confidence interval.

Item effects



Retest effect



Factor loadings

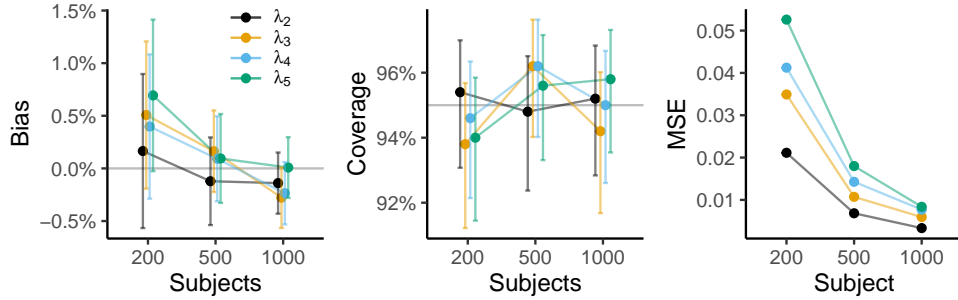


Figure 3: **Simulation results for parametric terms.** All points are averages over 500 Monte Carlo simulations, and error bars show 95% confidence intervals.

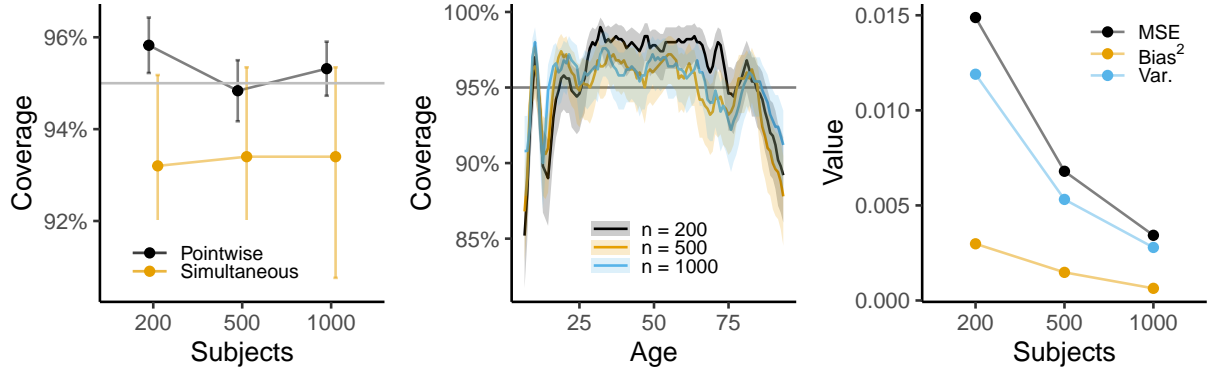


Figure 4: **Simulation results for smooth terms.** The left plot shows across-the-function coverage of pointwise confidence intervals and coverage of simultaneous confidence intervals. The center plot shows how coverage of pointwise intervals depends on age, and the right plot shows mean-square error, together with its bias-variance decomposition. Error bars and confidence bands represent 95% confidence intervals.

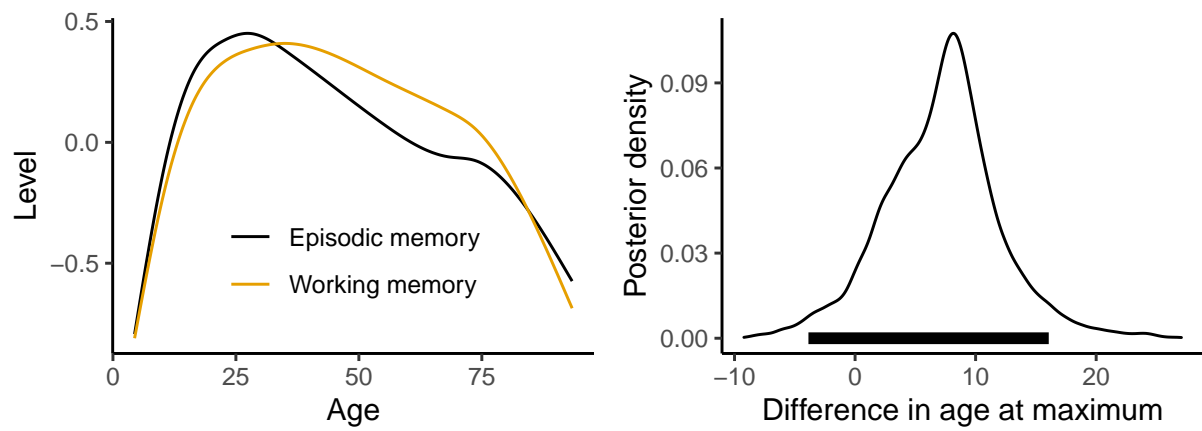


Figure 5: **Lifespan episodic and working memory.** Left: Estimated lifespan trajectories of episodic and working memory. Right: Empirical Bayes posterior distribution of the difference in age at maximum of episodic and working memory. Horizontal bar denotes 95% highest posterior density interval.

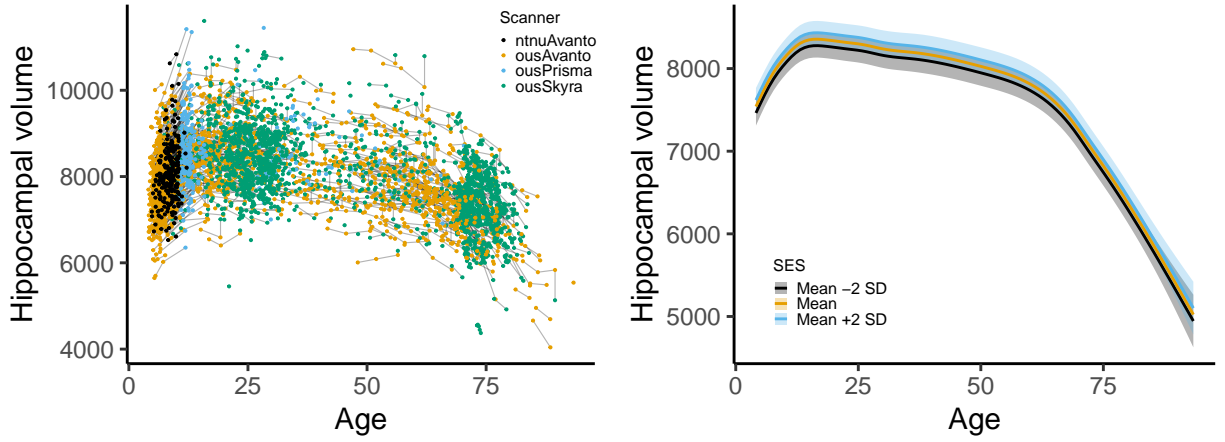


Figure 6: **Hippocampal volume curves.** Left: Total volumes of left and right hippocampus (in mm^3) plotted versus age. Repeated observations of the same individual are connected with gray lines. Right: Estimated hippocampal volume trajectories at mean socioeconomic status (SES) and at two standard deviation above or below mean. Shaded regions show 95% pointwise confidence intervals for SES two standard deviations above or below mean.

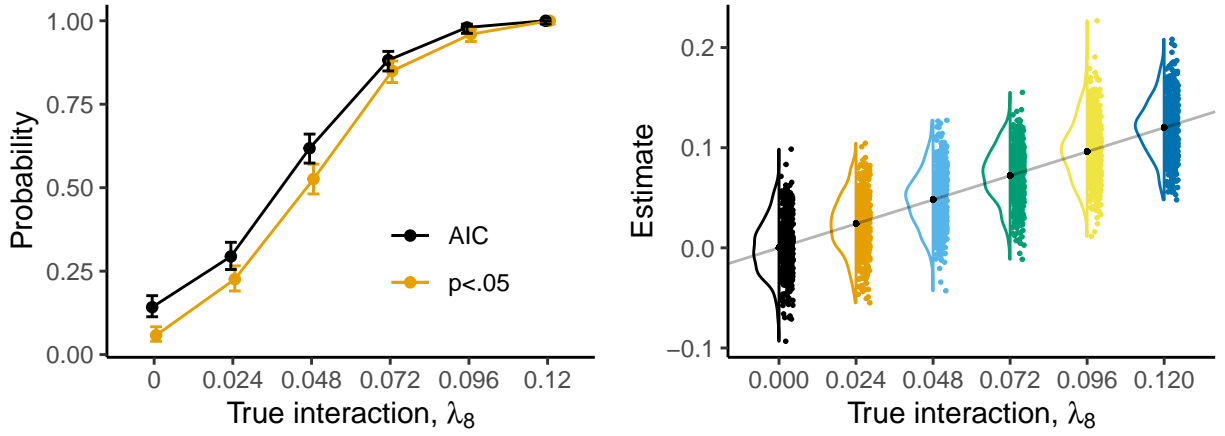


Figure 7: **Interaction term in latent covariates model.** Left: Probability of selecting a model containing an interaction term as a function of the magnitude of the interaction. 'AIC' denotes Akaike information criterion and ' $p < .05$ ' denotes selection based on testing $\lambda_8 = 0$ versus $\lambda_8 > 0$. Error bars show 95% confidence intervals. Right: Violin-dotplots (Hintze and Nelson, 1998) of estimated interactions for different values of the true interaction. Gray line and black points indicate the true values, and colored points indicate estimates in single Monte Carlo samples. Values are based on 500 Monte Carlo samples for each parameter combination.

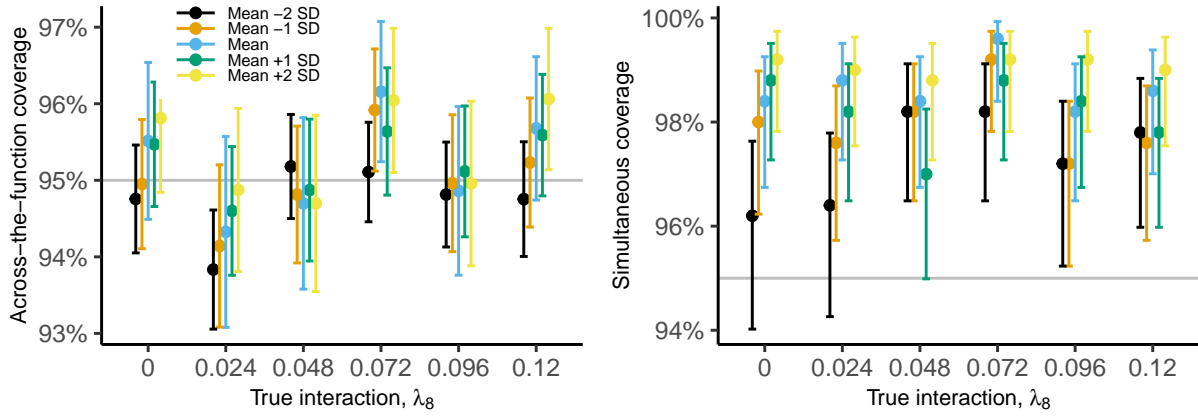


Figure 8: **Coverage of smooth terms in latent covariates model.** Across-the-function coverage of pointwise confidence intervals (left) and coverage of simultaneous confidence intervals (right) for five levels of latent socioeconomic status $\eta_1^{(2)}$. Intervals were computed with model (e), which contained a non-zero interaction term λ_8 .

List of Tables

1	Parameter estimates in latent response model. 'SE-naive' denotes standard error not taking uncertainty in factor loadings into account.	51
2	Comparison of models for the effect of socioeconomic status on hippocampal volume. AIC values have been shifted to be zero for the full model, for ease of comparison.	52
3	Parametric terms in model of hippocampal volume and socioeconomic status.	53

Table 1: Parameter estimates in latent response model. 'SE-naive' denotes standard error not taking uncertainty in factor loadings into account.

Parameter	Estimate	SE	SE-naive
<i>Item effects</i>			
β_{t2}	1.22	0.022	0.019
β_{t3}	2.05	0.031	0.026
β_{t4}	2.53	0.036	0.030
β_{t5}	2.89	0.040	0.032
<i>Retest effect</i>			
β_r	0.15	0.019	0.019

Table 2: Comparison of models for the effect of socioeconomic status on hippocampal volume. AIC values have been shifted to be zero for the full model, for ease of comparison.

Model	DF	Log-likelihood	AIC
(a): Free loadings	20	-5470	0.00
(b): (a) and no interaction, $\lambda_8 = 0$	19	-5471	-0.67
(c): Parents equal, $\lambda_1 = \lambda_2$ and $\lambda_4 = \lambda_5$	18	-5471	-1.28
(d): (c) and no interaction, $\lambda_8 = 0$	17	-5472	-1.91
(e): Item groups equal, $\lambda_1 = \lambda_2 = \lambda_3$ and $\lambda_4 = \lambda_5 = \lambda_6$	16	-5471	-5.18
(f): (e) and no interaction, $\lambda_8 = 0$	15	-5472	-5.84
(g): (f) and no main effect, $\lambda_7 = \lambda_8 = 0$	14	-5474	-4.56

'DF' denotes degrees of freedom.

Table 3: Parametric terms in model of hippocampal volume and socioeconomic status.

Parameter	Estimate	SE	SE-naive	Units
<i>Effects on hippocampal volume</i>				
Scanner ousAvanto, β_{h1}	-76.9	57.5	57.5	mm ³
Scanner ousPrisma, β_{h2}	76.1	65.2	65.2	mm ³
Scanner ousSkyra, β_{h3}	240	58.5	58.4	mm ³
Total intracranial volume, β_{h4}	0.00199	9.09E-05	9.09E-05	mm ³ /mm ³
Sex=Male, β_{h5}	220	33.1	33.1	mm ³
<i>Factor loadings</i>				
Education, $\lambda_1 = \lambda_2 = \lambda_3$	0.169	-	-	log(years)
Income, $\lambda_4 = \lambda_5 = \lambda_6$	0.265	0.0523	-	log(NOK)
Hippocampus, λ_7	58.2	32.4	-	mm ³
<i>Variance components</i>				
Socioeconomic status, $\sqrt{\psi_1^{(2)}}$	0.67	-	-	-
Hippocampus, $\sqrt{\psi_2^{(2)}}$	600	-	-	mm ³
Income residual, σ_1	0.595	-	-	log(NOK)
Education residual, σ_2	0.125	-	-	log(years)
Hippocampus residual, σ_3	133	-	-	mm ³

NOK denotes Norwegian kroner, with 10 NOK \approx 1 EUR. Scanner effects are relative to 'nt-nuSkyra', see Figure 6 (left). Units mm³/mm³ for total intracranial volume represent mm³ of hippocampus per mm³ of total intracranial volume.